frontiers in Marine Science

ORIGINAL RESEARCH
published: 19 March 2019
doi: 10.3389/fmars.2019.00115

Discovery of an Extensive Deep-Sea Fossil Serpulid Reef Associated With a Cold Seep, Santa Monica Basin, California

Magdalena N. Georgieva[1], Charles K. Paull[2], Crispin T. S. Little[3], Mary McGann[4], Diana Sahy[5], Daniel Condon[5], Lonny Lundsten[2], Jack Pewsey[3], David W. Caress[2] and Robert C. Vrijenhoek[2]*

[1] Department of Life Sciences, Natural History Museum, London, United Kingdom, [2] Monterey Bay Aquarium Research Institute, Moss Landing, CA, United States, [3] School of Earth and Environment, University of Leeds, Leeds, United Kingdom, [4] United States Geological Survey, Menlo Park, CA, United States, [5] NERC Isotope Geosciences Laboratory, British Geological Survey, Keyworth, United Kingdom

Multibeam bathymetric mapping of the Santa Monica Basin in the eastern Pacific has revealed the existence of a number of elevated bathymetric features, or mounds, harboring cold seep communities. During 2013–2014, mounds at ∼600 m water depth were observed for the first time and sampled by Monterey Bay Aquarium Research Institute's ROV *Doc Ricketts*. Active cold seeps were found, but surprisingly one of these mounds was characterized by massive deposits composed of fossil serpulid worm tubes (Annelida: Serpulidae) exhibiting various states of mineralization by authigenic carbonate. No living serpulids with equivalent tube morphologies were found at the site; hence the mound was termed "Fossil Hill." In the present study, the identity of the fossil serpulids and associated fossil community, the ages of fossils and authigenic carbonates, the formation of the fossil serpulid aggregation, and the geological structure of the mound are explored. Results indicate that the tubes were most likely made by a deep-sea serpulid lineage, with radiocarbon dating suggesting that they have a very recent origin during the Late Pleistocene, specifically to the Last Glacial Maximum ∼20,000 years ago. Additional U-Th analyses of authigenic carbonates mostly corroborate the radiocarbon dates, and also indicate that seepage was occurring while the tubes were being formed. We also document similar, older deposits along the approximate trajectory of the San Pedro Basin Fault. We suggest that the serpulid tube facies formed *in situ*, and that the vast aggregation of these tubes at Fossil Hill is likely due to a combination of optimal physical environmental conditions and chemosynthetic production, which may have been particularly intense as a result of sea-level lowstand during the Last Glacial Maximum.

Keywords: tubeworm, last glacial maximum, gas hydrate, vesicomyidae, Annelida, paleobiology, eastern Pacific, methane seep

OPEN ACCESS

Edited by:
Randi D. Rotjan,
Boston University, United States

Reviewed by:
Lorenzo Angeletti,
Istituto di Scienze Marine (ISMAR), Italy
Americo Montiel,
University of Magallanes, Chile

****Correspondence:***
Magdalena N. Georgieva
m.georgieva@nhm.ac.uk;
magdalena.n.georgieva@gmail.com

Specialty section:
This article was submitted to Deep-Sea Environments and Ecology, a section of the journal Frontiers in Marine Science

Received: *01 November 2018*
Accepted: *25 February 2019*
Published: *19 March 2019*

Citation:
Georgieva MN, Paull CK, Little CTS, McGann M, Sahy D, Condon D, Lundsten L, Pewsey J, Caress DW and Vrijenhoek RC (2019) Discovery of an Extensive Deep-Sea Fossil Serpulid Reef Associated With a Cold Seep, Santa Monica Basin, California. Front. Mar. Sci. 6:115. doi: 10.3389/fmars.2019.00115

INTRODUCTION

Cold seeps are remarkable marine environments characterized by the effluence of near ambient-temperature reduced fluids, usually rich in methane or hydrogen sulfide, from the seafloor. In recent years, information from autonomous underwater vehicle (AUV) surveys has greatly aided the discovery of cold seeps in the deep sea, which are recognized by the presence of patches of irregular

bathymetry in areas of otherwise undifferentiated sediment (Hovland and Judd, 1988; MacDonald et al., 2003; Wagner et al., 2013; Paull et al., 2015). Cold seeps often manifest as topographic mounds, pockmarks and outcrops of authigenic carbonates (Wagner et al., 2013), and are renowned for the often vast chemosynthesis-supported biological productivity that occurs at these sites compared to the otherwise generally food-limited deep sea. Cold seeps are also known to have been important habitats for deep-sea fauna throughout Earth's history since at least the Paleozoic (Peckmann et al., 1999b; Barbieri et al., 2004), and today, siboglinid tubeworms (Annelida), bathymodiolin mussels and vesicomyid clams (Bivalvia) thrive at seeps (Kiel, 2010), because they host chemoautotrophic endosymbionts that obtain nutrients from seeping fluids (Dubilier et al., 2008). The elevated productivity of cold seeps also provides habitats for a wealth of additional organisms that have not yet been found to possess such symbionts, such as fish, brachyuran crabs, polynoids, and serpulid tubeworms. The latter (Annelida: Serpulidae) are remarkable for their ability to form vast reef-like aggregations in shallow marine and brackish waters. While serpulids can occur in large numbers at deep-sea seeps (Olu et al., 1996a,b; Levin et al., 2012; Amon et al., 2017), they rarely construct sizeable reef structures below the photic zone. Here, we report on the discovery of, and investigations into, an unusually large accumulation of fossil serpulids within deep-sea waters that occurs in association with an active cold seep.

Serpulid worms are common in all marine environments, occurring from the intertidal down to hadal depths (Ippolitov et al., 2014), and possess an anterior end that terminates in a fan-like structure (crown) used for suspension-feeding (Kupriyanova et al., 2006). These annelids are easily recognized by their dwelling tubes, which are comprised of calcium carbonate and typically secured to a hard substrate. Members of this family are also notable for their gregarious behavior, amassing to form vast reefs by using the tubes of conspecifics as settlement substrate (ten Hove and van den Hurk, 1993). These worms can hence function as important ecosystem engineers, altering local hydrodynamics, and providing habitat structure utilized by other marine organisms (Schwindt et al., 2001), but can also accumulate to foul marine structures and modify ecosystems within which they are invasive. Large serpulid aggregations or reefs are commonly found in enclosed embayments of normal salinity or in brackish estuaries or lagoons (Bianchi et al., 1995). Conditions such as reduced competition for food and space, reduced predation, larval retention and possibly also high primary production are considered to promote reef formation behavior by serpulids, under which they can form reefs reaching tens of square meters in extent and over one meter in thickness (ten Hove and van den Hurk, 1993; Bianchi et al., 1995; Hoeksema and ten Hove, 2011). Although rare, there are also reports of serpulid reefs from deeper waters, such as serpulid-coral aggregations that were observed at depths of 450–650 m in the Adriatic Sea (Sanfilippo et al., 2013). In 1999, the discovery of an extensive reef comprised almost exclusively of the species *Serpula narconensis* at 91–105 m depth off the South Georgia continental shelf was reported, from where a single trawl collected over 1.5 tons of tubes made by this species (Ramos and San Martín, 1999). Serpulids have also been found to occur in high abundance within deep-sea cold seep environments (Vinn et al., 2013, 2014). Species of *Laminatubus* sp. are present in large numbers at the hydrothermal seeps of Jaco Scar on the Costa Rica convergent margin (Levin et al., 2012), and other serpulid species at cold seeps off northern Peru (Olu et al., 1996a), at the Barbados Accretionary Prism (Olu et al., 1996b) where they gather at high densities on concretions around mussel beds, and at seeps off Trinidad and Tobago (Amon et al., 2017). Within cold seeps, large serpulid populations are likely sustained by filter-feeding on the greater concentrations of organic matter in the water column at these sites, and have not yet been reported to possess microbial epi- or endo-symbionts.

Serpulid build-ups are also known from the fossil record, dating back to the Late Triassic (ten Hove and van den Hurk, 1993). One of the most extensive fossil serpulid reefs occurs at the Triassic-Lias boundary in southern Spain, in which a unit comprised mainly of tubes of the species *Filograna socialis* outcrops for 75 m and reaches 25 m in thickness. This reef is reported to have formed in deep water, but still within the photic zone (Braga and Lopez-Lopez, 1989). Large aggregations of tubes preserved in several fossil cold seep deposits have also been ascribed to the serpulids, such as the tube fossils of the Cretaceous Sada limestone (Nobuhara et al., 2008) and the Miocene Ca' Fornace and Marmorito carbonates of northern Italy (C.T.S. Little pers. obs.; Peckmann et al., 1999a; Kiel et al., 2018). In the Sada limestone deposit, the maximum observed thickness of the serpulid facies is greater than 6 m (Nobuhara et al., 2016). The identification of the serpulid species comprising fossil reefs can be problematic as the systematics of extant serpulids is based mainly on characteristics associated with the animals (Ippolitov et al., 2014). Nevertheless, a number of tube characteristics can be helpful such as tube aggregation, coiling/curving, attachment to substrate and external sculpture (see Ippolitov et al., 2014). Increasingly the ultrastructure of tubes is also used in relating fossil to recent taxa, in cases where the tube walls of fossil serpulids have not been significantly diagenetically altered (Vinn, 2005, 2008; Taylor and Vinn, 2006; Vinn et al., 2008a).

Multibeam bathymetric mapping of the Santa Monica Basin, southern California, has helped to reveal the existence of a number of elevated bathymetric features, or mounds, harboring cold seep communities (Normark et al., 2003; Hein et al., 2006). Exploration of these mounds using AUV-based 1-m resolution mapping and subbottom profiling, followed by ROV exploration and sampling, has revealed the presence of sub-surface gas hydrates. Paull et al. (2008) have hypothesized hydrate formation as a mechanism for mound uplift, while the proximity of some of the mounds to the trajectory of the San Pedro Basin fault system (Ryan et al., 2012) suggests that their formation may be associated with fault activity (Fisher et al., 2003; Gardner et al., 2003). During 2013–2014 Monterey Bay Aquarium Research Institute (MBARI) expeditions, an additional mound that had not previously been explored by remotely operated vehicle (ROV) was observed to be comprised predominantly of a large number of fossil serpulid tubes exhibiting various states of mineralization by authigenic carbonate. The mound was hence termed "Fossil Hill." In this study, results of extensive exploration of this

enigmatic mound are presented with the aim to characterize the physical and biological features of this anomalous structure, as well as to ascertain its mode of formation, and whether this is associated with fluid seepage.

MATERIALS AND METHODS

Seafloor Mapping and Sample Collection

High-resolution mapping and sub-bottom profiling surveys of selected topographic features within the Santa Monica Basin region were conducted in March 2013 using an AUV equipped with 400 kHz Reson 7125 multibeam sonar, 110 kHz chirp sidescan sonar, and a 1–6 kHz sweep chirp subbottom profiler (see Caress et al. (2008) for further methodological details). An objective was to explore along the inferred trace of the San Pedro Basin fault looking for the morphologies indicative of seafloor seepage sites (Paull et al., 2015), and evidence of recent movements along the fault (Ryan et al., 2012). AUV dives 20133006m1 and 20130311m1 revealed areas of anomalously rough seafloor both south or north of Santa Monica Canyon respectively, Fossil Hill being one of these (**Figure 1**). These areas were further explored during two ROV diving cruises of the R/V *Western Flyer* in May 2013 and June 2014. The AUV survey of the Fossil Hill site was repeated in April 2018 (AUV dive 201807m1) following improvement in processing software.

Samples were obtained from the Fossil Hill mound, as well as nearby seafloor exhibiting similar topography along the approximate axis of the San Pedro Basin Fault (**Figure 1**). Sample collection from these sites took place during seven dives of the ROV *Doc Ricketts*; DR476 and DR626-631 (**Supplementary Table S1**). The manipulator arms of the ROV were used to collect more heavily mineralized rock samples, while loose tube and bivalve shell rubble, as well as living bivalves, were collected using an ROV operated scoop and through push-coring (up to 22 cm long). A vibracorer mounted to the ROV was used to collect up to 165 cm long cores in areas of soft sediment. Push cores were extruded on board the ship, and all rock and fossil samples were subsequently rinsed in fresh water and dried, while live bivalves were preserved in 80% ethanol. Vibracores were logged, split, photographed and preserved at the United States Geological Survey, Menlo Park, CA, United States. **Supplementary Figure S1** shows locations of rock, vibracore, and push-core sampling at Fossil Hill. Video footage from a systematic ROV flight during DR627 was used to construct a video mosaic of a sub-region of the Fossil Hill mound (**Figure 1**). During this dive, the ROV was maintained ∼1 m above the seabed in order to collect multiple, overlapping parallel sweeps of video footage over the region of interest. Still images were later extracted from the video footage, and loaded into PhotoScan Pro (v. 1.1.6, Agisoft LLC) to build the mosaic.

Fossil Identification

Fossil serpulid tubes were photographed and imaged in greater detail using an Olympus SZH10 stereomicroscope. Five fragments of tubes from a range of diameters were also imaged using a Hitachi S-3400N-II variable pressure scanning electron microscope (SEM) at Moss Landing Marine Laboratories, CA, United States. Transverse and longitudinal broken surfaces of the tubes were mounted onto SEM stubs, gold coated, and observed using both secondary and backscatter electrons. The composition of four tube fragments was analyzed using fourier transform infrared spectroscopy (FTIR) to determine the form of calcium carbonate present in the tubes. Tubes were ground to a powder to incorporate material from all layers, and analyzed at Imperial College London, United Kingdom, in attenuated total reflectance mode. Additional fossil taxa associated with the fossil serpulid tubes were examined using a combination of light and scanning electron microscopy, using an FEI Quanta 650 FEG-ESEM at the University of Leeds, Leeds, United Kingdom. Identifications of associated taxa to the lowest possible taxonomic level were used to create a presence-absence matrix based on their occurrence within non-vibracore samples. Several non-parametric species richness estimators such as the incidence-based coverage estimator (ICE; Lee and Chao, 1994), and the iChao2 richness estimator; Chiu et al., 2014) were calculated using R (R Core Team, 2014; Chao et al., 2015). Authigenic carbonates from a subset of rock specimens were also prepared as thin sections to observe carbonate petrography.

Dating of Fossil Fauna and Authigenic Carbonates

Eight tube and bivalve fragments not cemented by methane-derived authigenic carbonates (MDAC, Paull et al., 1992) were selected for radiocarbon analysis. These were cleaned to ensure removal of attached debris and mineralization using the following technique: cleaning using paintbrush and fresh water, placement in an ultrasonic bath for 5 min, suspension in weak hydrochloric acid (0.25 N HCl) for 2 min, placement in distilled water in an ultrasonic bath for 5 min, drying in an oven at 50°C for ∼1 h. Radiocarbon measurements were obtained by accelerator mass spectrometry (AMS) at the National Ocean Sciences Accelerator Mass Spectrometry (NOSAMS) facility, Woods Hole Oceanographic Institution, MA, United States. The radiocarbon ages were obtained by a $^{14}C/^{12}C$ ratio using a ^{14}C half-life of 5,568 years (Stuiver and Polach, 1977). The raw radiocarbon ages were then converted to calibrated calendar ages (cal yr B.P.) using the CALIB 7.1 program (Stuiver et al., 2018). The calibrated ages are reported as the peak probability ages and the 2 sigma ranges are also included (**Table 1**). A reservoir age of 1750 year was applied to the worm tubes and mollusks following Mix et al. (1999) because they occupied the same substrate as bottom-dwelling (benthic) foraminifera.

The above cleaning steps were performed to minimize any effect of old carbon from seepage fluids on radiocarbon dates (Paull et al., 1989; Pohlman et al., 2011), while for samples affected by obvious MDAC mineralization, U-Th dating was used in order to eliminate any age bias from old carbon. MDAC cements present on the outer walls of serpulid tubes and bivalve shells, as well as infilling serpulid tubes, were dated using this technique at facilities at the NERC Geochronology and Tracers Facility, British Geological Survey, United Kingdom, following the analytical protocol outlined by

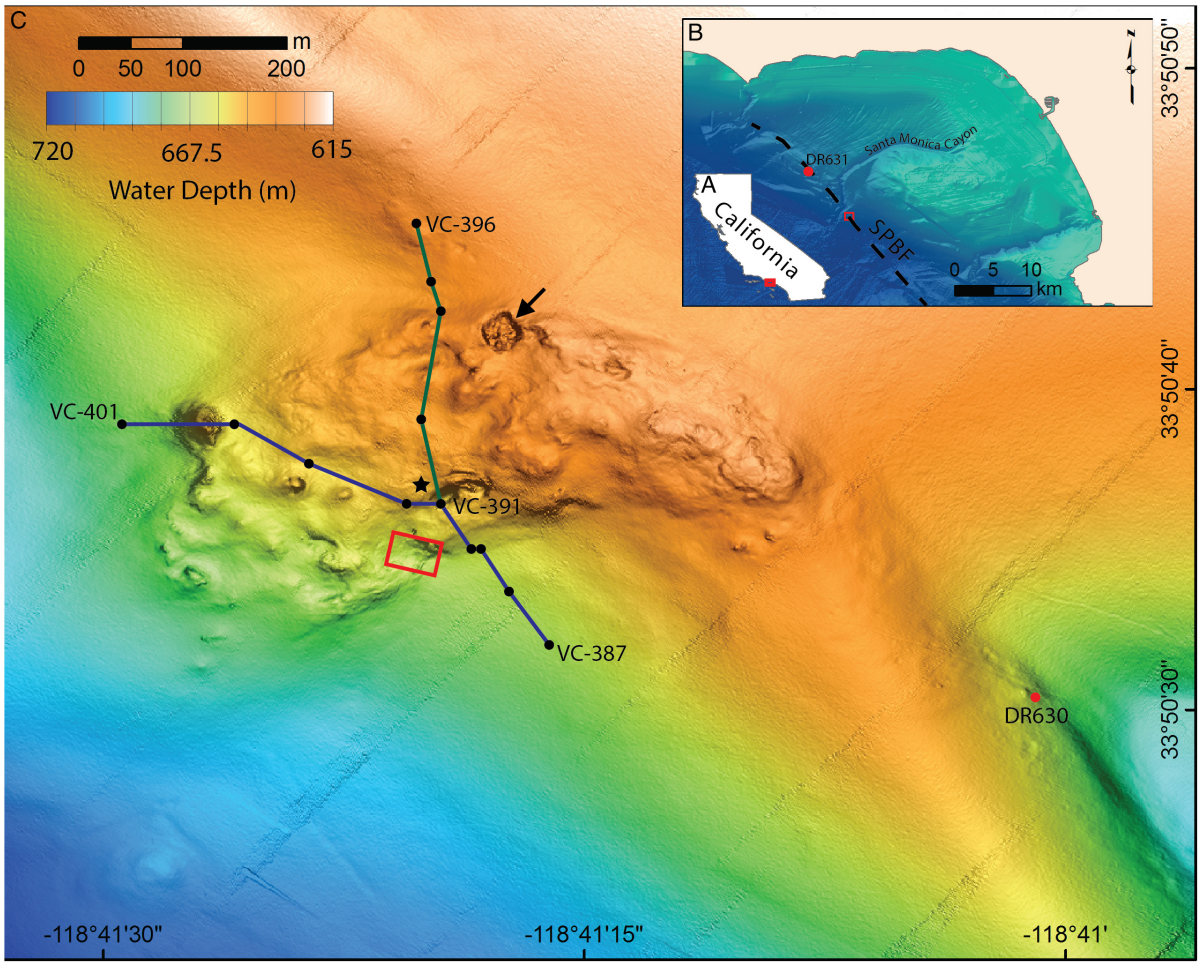

FIGURE 1 | Location and bathymetry of Fossil Hill. **(A)** Map of California showing the location of the Santa Monica Bay area, red box shows area pictured in **B**. **(B)** Santa Monica Bay showing the location of Fossil Hill (red box, pictured in detail in **C**) in relation to the Santa Monica canyon and the approximate position of the San Pedro Basin fault (SPBF, dashed black line; Ryan et al., 2012). The location of the sampling site northeast of Fossil Hill (DR631) is also shown. **(C)** Detailed bathymetry of the Fossil Hill mound. Blue and green lines show the tracks of the elevation profiles in **Figure 6**. The black dots within these tracks represent individual vibracore locations, with start, and end vibracore numbers labeled. Red box shows area in which video-mosaic (**Figure 3**) was performed. Black star denotes the location of an extensive live clam and bacterial mat bed, and a large pockmark (27 m wide, 4 m deep) on the northern margin is indicated with an arrow. The sampling site southeast of Fossil Hill (DR630) is labeled.

Crémière et al. (2016). Additional carbon ($\partial^{13}C$) and oxygen ($\partial^{18}O$) isotope measurements conducted at the above facility were also used to confirm whether Fossil Hill carbonates are methane-derived **(Supplementary Table S2)**.

Age interpretation of U-Th isotope data from MDAC requires a correction for the amount of initial ^{230}Th incorporated into the carbonate either via the inclusion of detrital material or through adsorption of Th from the decay of dissolved U in the water column onto particle surfaces. In order to determine a site-specific correction for Fossil Hill, the U-Th composition of five sediment samples from four vibracores collected during dive DR630 was analyzed. Unfortunately, the sediment samples proved unsuitable for the purpose of determining an initial ^{230}Th correction, as their measured ($^{234}U/^{238}U$) activity ratios were greater than 1, indicating the presence of young $CaCO_3$ of either biogenic or authigenic origin. Instead, the initial ^{230}Th correction used for the Fossil Hill MDAC was interpolated for a water depth of 650 m based on U-Th measurements of carbonate-free sediment samples from Baltimore Canyon (ca. 400 m depth) and Norfolk Canyon (ca. 1600 m depth) on the US Atlantic margin (Prouty et al., 2016). All U-Th data are listed in (**Supplementary Table S3**), with a selection of dates considered accurate presented in **Table 2**.

RESULTS

Characteristics of Fossil Hill and Associated Carbonate Deposits

The AUV surveys reveal that Fossil Hill has a lobate shape which is approximately 500 m long and 270 m at its widest extent (**Figure 1C**). Fossil Hill is positioned on seafloor which gently

TABLE 1 | Radiocarbon (^{14}C) dates of Fossil Hill bivalve shells and serpulid tubes.

NOSAMS accession number	Sample reference	Sample description	Radiocarbon age (^{14}C yrs BP)	Error	$\delta^{13}C_{VPDB}$ (‰)	Minimum calibrated age (cal yrs BP) 2 sigma	Maximum calibrated age (cal yrs BP) 2 sigma	Mean calibrated age (cal yrs BP) 2 sigma
OS-121607	DR476 A-1	*E. elongata* bivalve shell	1,260	20	−1.4	Recent	Recent	Recent
OS-121608	DR627 BIO-2	*P. soyoae* bivalve shell	21,100	60	1.06	23,037	23,540	23,294
OS-121623	DR476 A-1	Serpulid tube	22,300	65	−18.06	24,437	25,047	24,729
OS-121624	DR626 PSC-66	Serpulid tube	21,500	60	−11.11	23,550	24,006	23,778
OS-121626	DR626 R-4	Serpulid tube	21,500	55	−12.26	23,556	24,001	23,778
OS-121625	DR627 PSC-53	Serpulid tube	21,800	60	−14.88	23,898	24,321	24,108
OS-121742	DR629 VC-400 (159–163 cm depth)	Serpulid tube	21,800	120	−12.87	23,799	24,420	24,110
OS-121743	DR629 VC-400 (159–163 cm depth)	Serpulid tube	22,400	130	−12.98	24,456	25,264	24,863
OS-113658	DR629 VC-400 (160–162 cm depth)	Serpulid tube	22,300	80	−13.01	24,419	25,077	24,733

All samples were analyzed using hydrolysis and all radiocarbon results were corrected for isotopic fractionation using unreported $\delta^{13}C$ values measured on the accelerator. $\delta^{13}C$ values are reported relative to the VPDB standard.

TABLE 2 | U-Th composition and age interpretation of Fossil Hill methane-derived authigenic carbonate (MDAC) samples and shells and tubes.

Sample reference	Sample description	^{238}U (ppm)	^{232}Th (ppm)	$^{230}Th/^{232}Th$	$^{234}U/^{238}U$	U-Th age (corr. ka BP)
DR626 R-1 A	MDAC infill of serpulid tube	12.2	1.697	7.2	1.1471 ± 0.021	31.7 ± 2.9
DR626 R-2 C	MDAC infill of serpulid tube	13.4	1.908	8.8	1.1513 ± 0.022	43.4 ± 2. 9
DR626 R-4 A	MDAC infill of serpulid tube	10.1	3.228	3.6	1.1396 ± 0.051	30.9 ± 7.1
DR626 R-4 B	MDAC surrounding tube	6.4	1.168	3.8	1.1320 ± 0.028	17.4 ± 3.8
DR626 R-4 C	MDAC infill of serpulid tube	4.3	0.947	3.7	1.1371 ± 0.034	20.6 ± 4.6
DR627 R-4 tube 1	Serpulid tube	58.0	0.287	118.8	1.1416 ± 0.002	20.1 ± 0.1
DR627 R-4 tube 2	Serpulid tube	38.2	0.616	37.7	1.1470 ± 0.003	20.3 ± 0.3
DR627 shell 1 B	*P. soyoae* bivalve shell	1.0	0.049	10.7	1.1495 ± 0.007	16.1 ± 0.8
DR627 shell 2 A	*P. soyoae* bivalve shell	2.8	0.175	8.8	1.1465 ± 0.008	17.0 ± 1.1
DR627 shell 2 B	*P. soyoae* bivalve shell	2.6	0.102	13.7	1.1471 ± 0.005	17.2 ± 0.7
DR628 R-5 A	MDAC cementing bivalve shells	3.1	0.055	13.7	1.1470 ± 0.003	7.1 ± 0.4
DR628 R-5 B	MDAC cementing bivalve shells	3.7	0.044	19.5	1.1485 ± 0.002	7.1 ± 0.2
DR629 R-3 1/2 A	MDAC surrounding tube	2.0	0.047	27.2	1.1499 ± 0.004	21.3 ± 0.5
DR629 R-3 2/2 A	MDAC surrounding tube	2.5	0.034	43.1	1.1478 ± 0.004	19.0 ± 0.3
DR629 R-3 1/2 B	MDAC infill of serpulid tube	2.9	0.067	22.2	1.1454 ± 0.003	16.5 ± 0.5
DR629 R-3 2/2 B	MDAC surrounding tube	2.7	0.065	24.4	1.2326 ± 0.016	17.6 ± 0.5
DR630 R-3 B	MDAC cementing bivalve shells	3.4	0.101	21.2	1.1459 ± 0.005	20.8 ± 0.6
DR630 R-4 A	Late-stage cement, MDAC with serpulid tubes	1.3	0.125	17.2	1.1342 ± 0.009	31.7 ± 1.1

Uncertainties are ±2s (abs).

slopes to the south-west with the highest elevation reaching 622 m depth, and extending down slope to 672 m depth. The surface of Fossil Hill is 5–15 m higher than the surrounding seafloor with an overall uneven appearance, punctuated by discrete circular depressions and topographic highs. The roughly circular depressions range from a few meters to 27 m in diameter, the latter being a ∼4 m deep sinkhole or pockmark which occurs on the northern margin of Fossil Hill (**Figure 1C**, arrowed). The circular topographic highs are less than 50 m in diameter and up to 6 m high. The seafloor lineation that is interpreted as the approximate trace of the San Pedro Basin fault (Ryan et al., 2012) runs very close (∼50 m) to the eastern edge of Fossil Hill (**Figure 1B**). Sub-bottom chirp profiles across both Fossil Hill and the site 290 m to the southeast show a strong seafloor reflection where the carbonate rocks are exposed on the seafloor. Fossil Hill is positioned on top of a ridge-like tectonic feature (**Figure 2**), and appears to have formed on the eroded crest of this ridge where accumulating sediment was thin or absent. A thin drape of sediment seems to have covered the northern and southern ends of Fossil Hill, while reflectors passing under the deposit indicate that it is less than 5 m thick (**Figures 2A–A',D–D'**). On the flanks of Fossil Hill, the strong reflector dives into the subsurface and is onlapped by a package of finely layered reflectors that are up to 45 m thick (**Figures 2C–C'**). This geometry reveals that the Fossil Hill deposit and the southeastern outcrop continue into the subsurface.

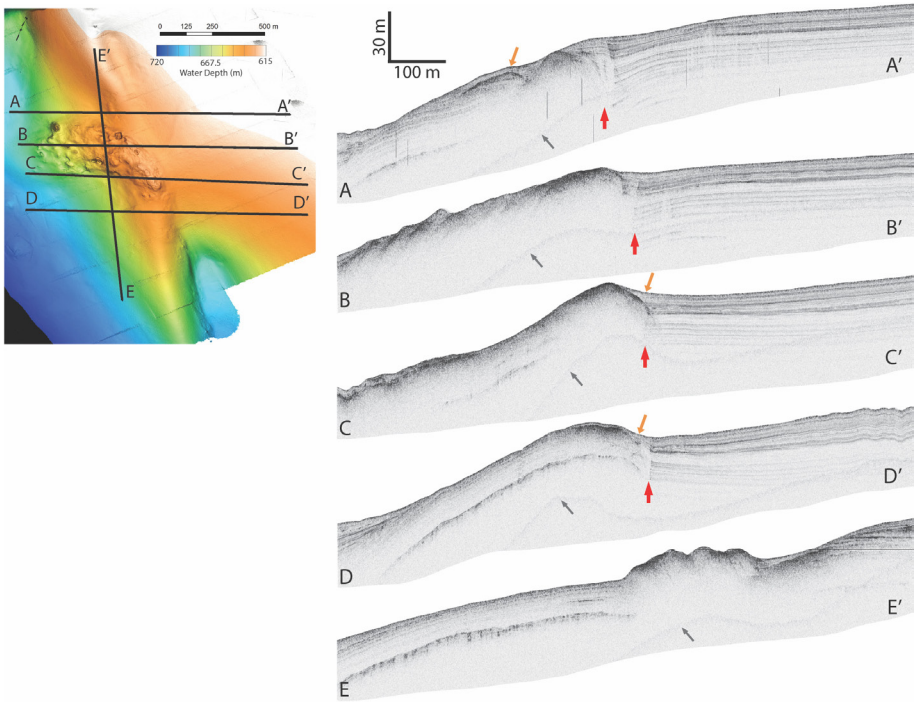

FIGURE 2 | Chirp profiles taken across the Fossil Hill main mound structure. Colored insert shows the locations of the paths of profiles **A–A'**, **B–B'**, **C–C'**, **D–D'**, **E–E'**. The locations of recent fault offsets (red arrows), sediment drape covering or lapping onto the mound (orange arrows), and artifacts associated with a multiple reflection off the sea surface (gray arrows) are shown.

The ROV surveys show that large slabs or blocks of carbonate rock are exposed between areas of sediment drape on the surface of Fossil Hill (**Figure 3**). The carbonate rocks are separated by cracks and gullies, and holes at the bases of these reveal >10 cm high open cavities underneath the slabs (**Figure 3**). The large pockmark to the north of Fossil Hill (**Figure 1C**) is rimmed by large flattened carbonate slabs that at multiple locations are sloping into the crater (**Figure 4A**), and the crater floor is littered with boulders that appear to be a former carapace that has fallen into the depression.

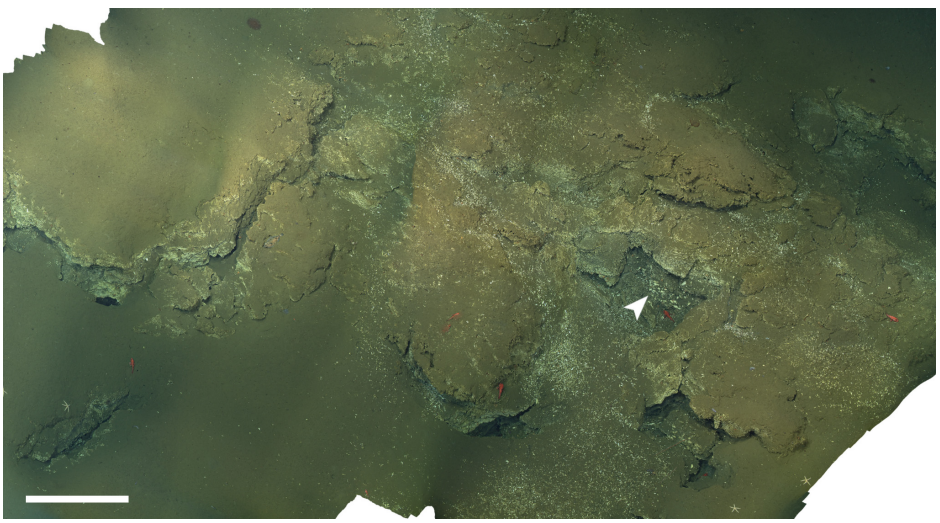

FIGURE 3 | Video-mosaic of a section of Fossil Hill (area shown in **Figure 1C**). White arrow head shows locations of the depression with overhang figured in more detail in **Figure 4E**, scale bar is approximately 2 m.

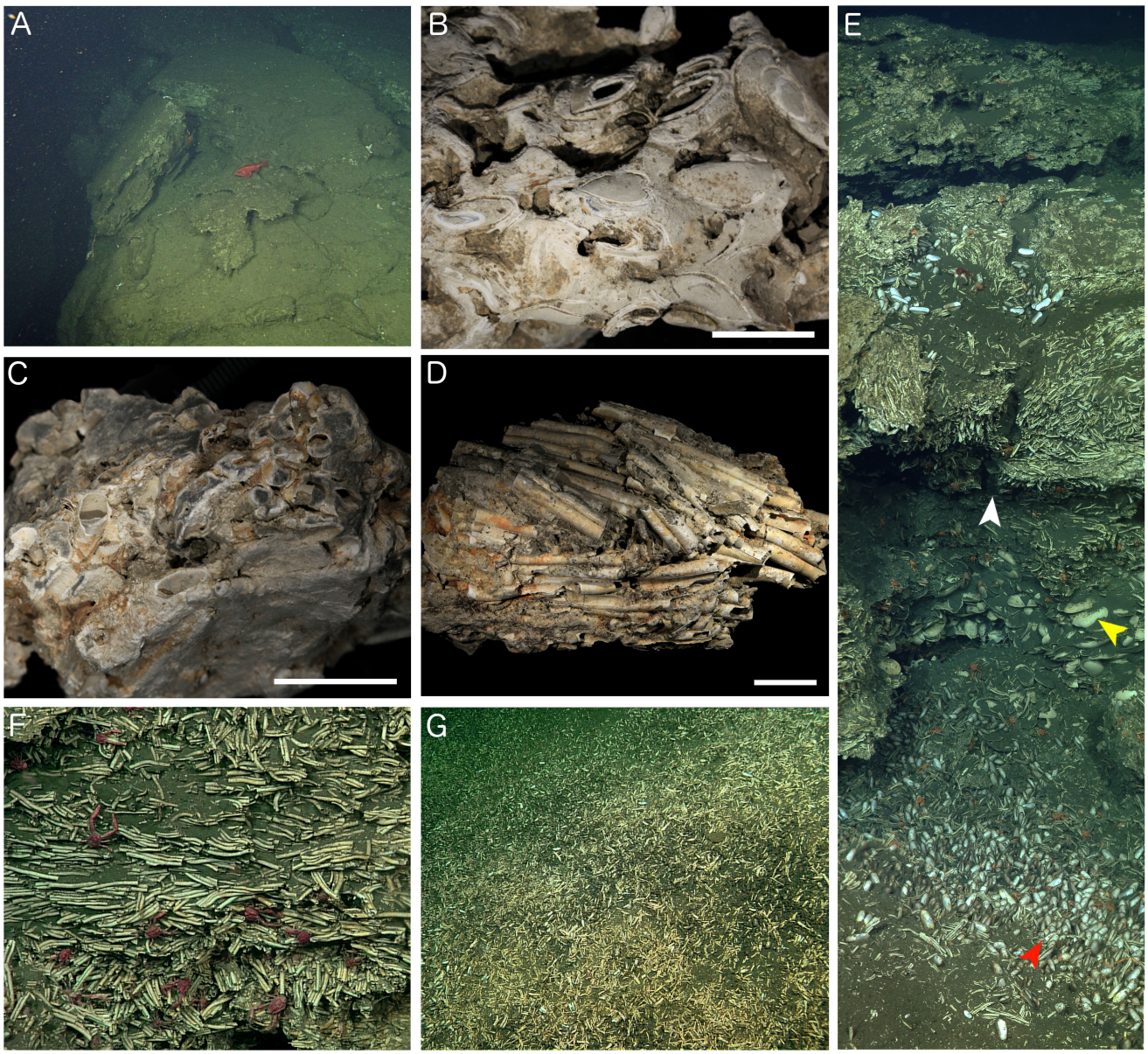

FIGURE 4 | Characteristics of Fossil Hill. **(A)** Large carbonate slabs on the edge of large pockmark structure (**Figure 1C**) which appear to be sliding into the hole (hole is to the left in the image). **(B)** Carbonate rock recovered south of the main Fossil Hill mound containing many preserved bivalves, sample DR630 R-3, and scale bar is 20 mm. **(C)** Fossil Hill carbonate with embedded worm tubes, sample DR629 R-2, and scale bar is 20 mm. **(D)** Densely packed and aligned tube fragments that are only weakly cemented by carbonate, DR626 R-4, and scale bar is 20 mm. **(E)** Mosaic of the wall of a small depression pictured in **Figure 3**, showing interlayered fossil worm tubes and bivalve shells. Perspective of **F** (white arrow), large bivalve shells (yellow arrow), and smaller living bivalves (red arrow) are highlighted. **(F)** Detail of the fossil worm tubes from the depression in **E** (white arrow), showing that they are only weakly cemented together and are aligned in parallel. Red munidopsid squat lobsters were common. **(G)** Slope on the southern side of Fossil Hill littered with tube and bivalve hash.

Neither gas bubbles or gas hydrates were observed during the ROV explorations.

The majority of samples of authigenic carbonate rock from Fossil Hill contained fossil serpulid worm tubes as well as bivalve and gastropod shells (**Figures 4B–D** and **Supplementary Table S1**), held together with variable amounts of carbonate cement comprised of isopachous fibrous aragonite (**Figure 5**). Most rock samples primarily contained worm tubes. The worm tube-dominated samples exhibited variable degrees of cementation, ranging between rock exhibiting many tubes filled with carbonate cement and strongly cemented together (**Figure 4C**) to weakly cemented tubes (**Figure 4D**). Tubes within rock samples also exhibited altering orientations, at times being mostly aligned in parallel (**Figures 4D,F**). Bivalve and gastropod shells rarely dominated carbonate rock faunal content (**Figure 4B**). The authigenic carbonate cements comprised a

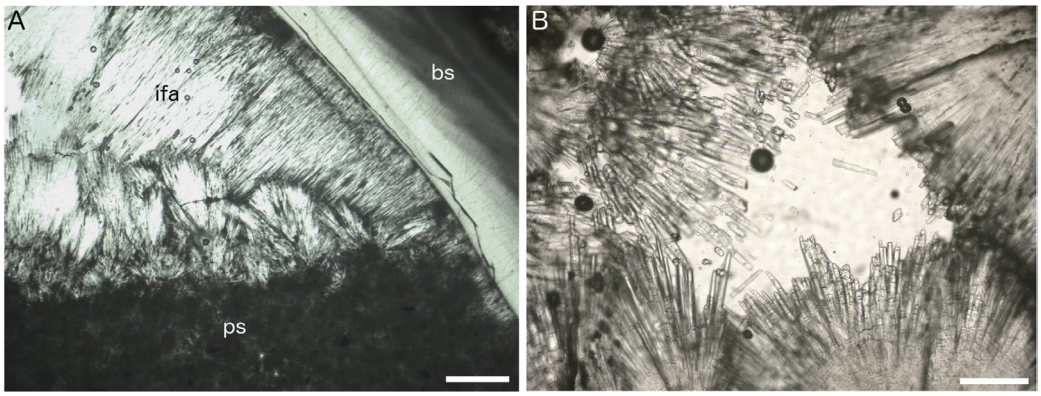

FIGURE 5 | Petrographic thin section images of Fossil Hill seep carbonates. **(A)** Isopachous fibrous aragonite cement (ifa) and peloidal micritic sediment (ps) forming geopetal fill within shelter cavity formed by articulated vesicomyid bivalve shell (bs), plain polarized light, sample DR630 R-3, and scale bar is 200 μm. **(B)** Detail of isopachous fibrous aragonite crystals, plain polarized light, sample DR629 R-5, and scale bar is 80 μm.

variable proportion of dark micrite, sometimes with distinct peloids (**Figure 5A**), and isopachous fibrous aragonite, often growing into open spaces within serpulid tubes and articulated bivalve shells (**Figures 5A,B**). In these cases the micritic cements obviously formed before the aragonite cements. In some serpulid worm tube-rich samples, they occurred as geopetal structures, indicating the tubes were horizontal to the palaeo-seafloor while they were being mineralized and after the death of the worms forming them. This was evident in the orientation of some the tubes in **Figure 4F**. Many of the carbonate rock samples were heavily corroded (e.g., **Figures 4B,C**) and had a chalky texture. Further, some had iron and manganese-rich crusts on the surfaces exposed to seawater, indicating they had been present on the seafloor for a considerable period of time. In addition, encrusting organisms were present on some of the samples, including bryozoans (*Schizoporella* species), small serpulids and sponges.

A worm tube-rich deposit was especially evident within one of the depressions encountered with the ROV (**Figures 3**, **4E**), in which a large proportion of the walls were exclusively built up of loose worm tubes aligned in parallel to each other (**Figure 4F**). These tubes were positioned on top of a layer of large bivalve shells with a shell length of up to 100 mm, while the base of the depression contained smaller, living bivalves with a shell length of up to 48 mm (**Figure 4E**, see section "Taxa Associated With the Fossil Serpulids"). Worm tube and bivalve shell rubble was also found to be eroding from these loosely consolidated deposits, and to be flowing down slopes (**Figure 4G**) as well as collecting within depressions. Vibracores collected in areas of soft sediment on Fossil Hill revealed that in some areas, depths of over 1 m of tube rubble had accumulated (**Figure 6** and (**Supplementary Table S1**) which were generally overlain by bivalve shell rubble, however tubes and bivalves were mixed together in a number of the cores. While the tubes were very abundant throughout Fossil Hill, no live animals were found within the tubes and no live bivalves with a shell length of up to 100 mm and pictured in **Figure 4E** were observed. Living bivalves (shell length of up to 48 mm) were abundant at Fossil Hill, occurring in depressions between carbonate slabs (**Figure 4E**), and colonizing an extensive patch at high densities at which they were also overgrown by bacterial mats (location shown in **Figure 1**). Subsequent morphological and molecular investigations showed that the living bivalves are predominantly the vesicomyid species *Ectenagena elongata*. Indications of the local reworking of the Fossil Hill deposit, and the presence of living bivalves in depressions (e.g., **Figure 4E**), appear to disrupt stratigraphic order at the site, and hence make it difficult to derive age relationships from stratigraphy.

Two other regions identified as elevated areas of rough topography in the 1-m bathymetric grids lying along the axis of the San Pedro Basin Fault were also visited during ROV dives DR630 and DR631 (**Figure 1**). They were found to have similar deposits consisting of fossilized serpulid tubes, bivalves and gastropods entombed within authigenic carbonates. The first (visited on ROV dive DR630) is a ∼5 m outcrop with >1 m of relief in 660 m water depth, located 290 m to the southeast of Fossil Hill on the flanks of the ridge (**Figure 1C**). The other (DR631) is within a ∼1.6 km long and >350 m wide area located 7.9 km northwest of Fossil Hill on the north side of Santa Monica Canyon in 509–530 m water depths, and lying on the extension of the same ridge (**Figure 1B**). The carbonate rock samples from these two sites generally contained fewer serpulid tubes and much less authigenic aragonite cement than the Fossil Hill samples, with these cements forming thin veins within often siliciclastic-rich micrites. The exposed surfaces of many of the DR630 and DR631 samples were heavily corroded and bored by *Polydora* sp. annelid worms. They were often also encrusted by bryozoans (including *Haywardipora* cf. *orbicula* and *Schizoporella* species), small serpulids, hydroids and sponges. These are all indications of long seafloor exposure.

Fossil Hill Paleo-Community

Fossil Serpulid Tubes

No complete worm tubes were found, however, the lack of diagenetic alteration of many of the Fossil Hill tube fragments enabled their morphology to be assessed in detail. The tubes either occurred singly, or more commonly as two or more

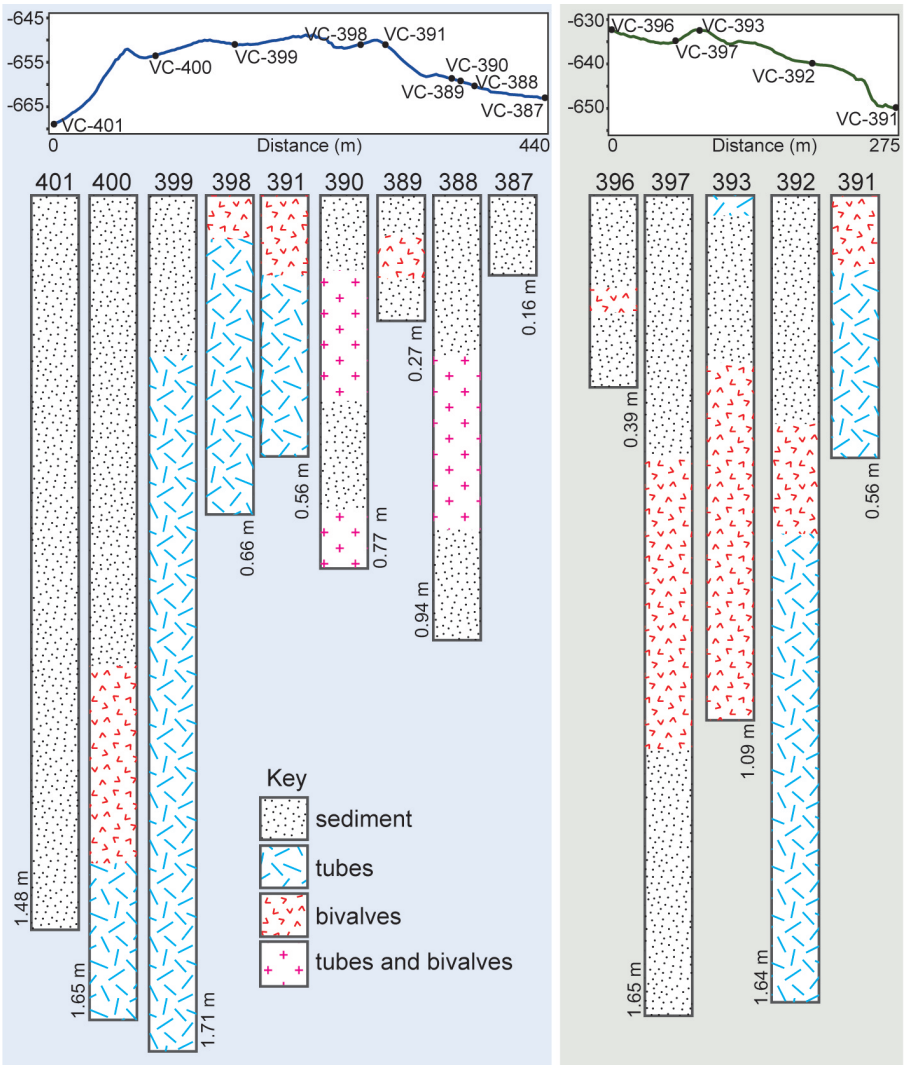

FIGURE 6 | Elevation profiles through parts of Fossil Hill along which vibracores were collected, and contents of cores (78 mm diameter) collected along the above profiles. Annotations on cores show core depths in meters, and sediment refers to fine-grained hemipelagic sediment. Tracks along which elevation profiles were created are illustrated in **Figure 1C**.

attached to each other along a longitudinal edge (**Figures 7A,B**). The majority of fragments were straight with only occasional strongly sinuous tubes observed (**Figures 7A,B**) and were generally circular or near-circular in cross-section. The tubes ranged from 1 to 7 mm in diameter (mean = 3.5 mm, n = 219; (**Supplementary Table S1**), very small tubes up to 1 mm in diameter were occasionally observed, and several were found attached to larger tubes (**Figure 7C**). The outer tube walls exhibited a texture of closely spaced, fine transverse wrinkles or growth-lines, that were more obvious in a subset of the tubes, and also appeared to be present in the tube layer below the outermost (**Figure 7D**). Many of the tubes also contained a single distinct undulating keel on their outer surfaces (**Figures 7A,E**), as well as peristomes, or occasional thickenings of short transverse sections of the tube wall (**Figure 7F**). Intricate ribbed calcareous tabulae were also found inside a subset of the tubes (**Figure 7G**). The above morphological characteristics were generally shared across the majority of tube fragments observed from Fossil Hill.

Analysis of the ultrastructure of the tubes (**Figure 8**) revealed them to be comprised of two distinct layers – a fine-grained inner layer and a coarser-grained outer layer (**Figure 8A**). The innermost tube layer was composed of acicular crystallites approximately 5 μm in length, arranged in multiple orientations and known in serpulid tubes as an irregularly oriented prismatic (IOP) tube ultrastructure (**Figure 8B**). This texture continued further into the tube wall, where it was partially mixed with homogeneous carbonate cement (**Figure 8C**), or was in patches replaced by a grainy texture that is either primarily comprised of homogeneous cement, or is a recrystallized version of

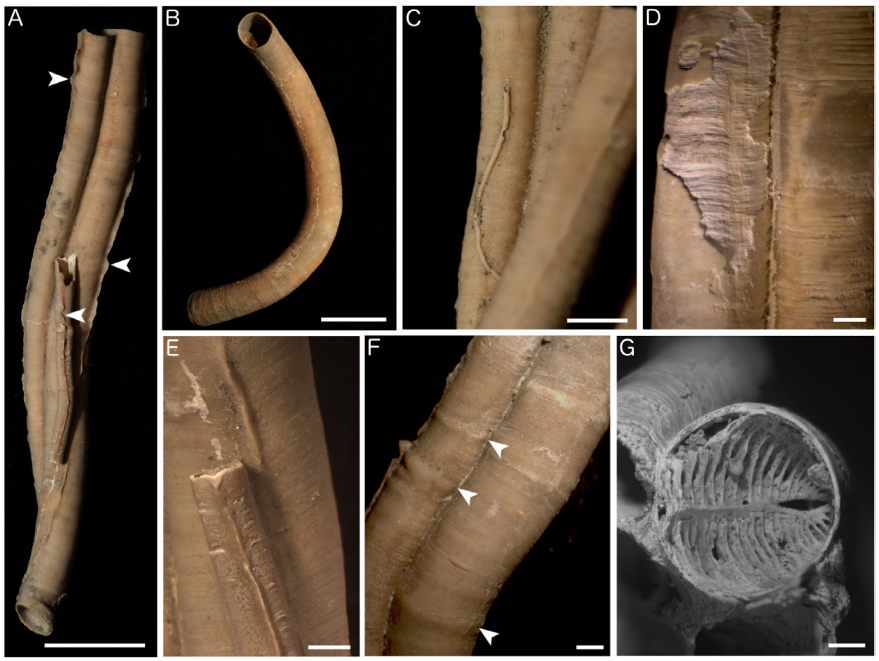

FIGURE 7 | Morphology of Fossil Hill serpulid tubes. **(A)** Several attached tube fragments with keels (white arrows) showing gregarious growth, sample DR476 A-1, and scale bar is 10 mm. **(B)** Curved nature of some of the fragments, sample DR629 PSC-52, and scale bar is 10 mm. **(C)** Small tube attached to larger tube, sample DR626 PSC-66, and scale bar is 2 mm. **(D)** Detail of transverse wrinkles apparent on some outer tube surfaces which are also present in the tube layer beneath the outermost, sample DR476 A-1, and scale bar is 1 mm. **(E)** Detail of tube keels, sample DR476 A-1, and scale bar is 1 mm. **(F)** Detail of peristomes occasionally present on the tubes (white arrows), sample DR476 A-1, and scale bar is 1 mm. **(G)** Detail of a tabula inside one of the tubes, sample DR476 A-1, and scale bar is 1 mm.

the irregularly oriented prismatic texture in **Figures 8B,C**. Longitudinal sections of tubes also revealed that the irregularly oriented prismatic texture was more intact toward the inside of the tube wall, and becomes increasingly homogeneous in nature toward the outer tube wall (**Figure 8E**). The crystals of the outer tube wall are approximately 25–30 μm in length and represent a spherulitic prismatic structure (SPHP) (**Figure 8F**). Comparison to established FTIR spectra for calcite and aragonite as well as mixtures of the two forms (Loftus et al., 2015) revealed that the Fossil Hill serpulid tubes to be predominantly comprised of calcite (based on the absence of a double peak at the 711 and 700 cm^{-1} wavelength positions; see **Supplementary Figure S2**).

We interpret all of the tubes as belonging to the same species, as significant differences between them were not observed (smaller differences could be due to intraspecific variation and the observed presence of a range of ontogenic stages), and as dense serpulid settlement is often dominated by a single taxon. The long, straight sections of the Fossil Hill serpulid tube fragments are typical of dense settlement of these annelids, which often results in tubes growing in an upright position away from their settlement substrate and leads to parallel erect tube morphologies (ten Hove, 1979). Gregarious behavior and reef formation is commonly observed in serpulid genera such as *Hydroides*, *Ficopomatus*, and *Serpula*, all of which are known from the eastern Pacific (Bastida-Zavala, 2008), however, generally not from deep waters. The size of the Fossil Hill tubes is consistent with those made by *Serpula* and *Protula*, however *Serpula* tubes commonly have funnel-shaped peristomes (Ippolitov et al., 2014; **Figures 2F,G**) which were not observed on any of the Fossil Hill tubes, and *Protula* tubes from the region do not have peristomes (Reish and Mason, 2003). The species *Serpula columbiana* is described from the west coast of North America and thus locally to Fossil Hill, but *S. columbiana* tubes also notably lack the longitudinal keels observed on the Fossil Hill tubes (Kupriyanova, 1999). In addition, the ultrastructure of the tubes of three *Serpula* species examined by Vinn et al. (2008b) does not match that of the Fossil Hill tubes.

Deep-sea serpulid genera include *Bathyvermilia*, *Neovermilia* and *Laminatubus*, and the occurrence of the Fossil Hill tubes in deep water, their presence in great numbers, as well as and the undulating keel observed on the larger tube fragments from Fossil Hill, are features more consistent with genera such as *Neovermilia* and *Laminatubus* which can also have similar keels and can occur in vast numbers at deep-sea sites of organic enrichment (E. Kupriyanova *pers. comm.*). The tube ultrastructure presented by the Fossil Hill tubes of an inner IOP layer and an outer SPHP layer, as well as their calcite composition, is also observed in *Laminatubus alvini* tubes (ten Hove and Zibrowius, 1986). The latter species is described from eastern Pacific hydrothermal vents and can have substantial unattached tube portions with a circular cross-section, however, comparison of these sections with those of Fossil Hill tubes revealed differences in the smoothness of the outer tube wall, as well as degree of undulation of the keels. *Neovermilia* has

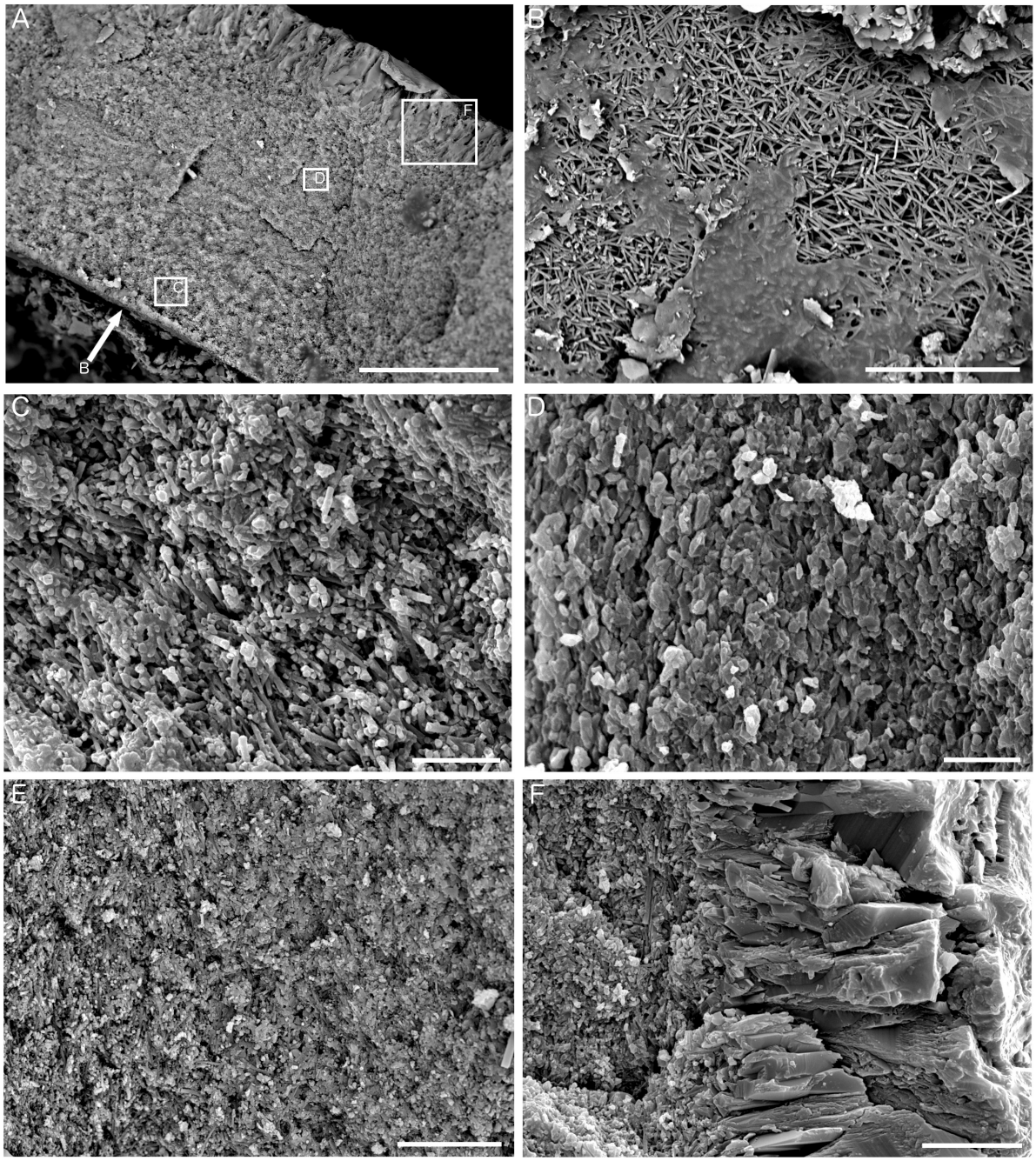

FIGURE 8 | Ultrastructure of Fossil Hill tubes. **(A)** Transverse section of a tube showing fine-grained inner layer and coarse-grained outer layer, sample DR476 A-1, and scale bar is 50 μm. Arrow shows perspective of **B**, and boxes show representative locations for the textures pictured in **C**, **D**, and **F**. **(B)** View looking down onto the inner tube surface showing irregularly oriented prismatic (IOP) ultrastructure comprised of crystallites approximately 5 μm in length, sample DR626 R-4, and scale bar is 20 μm. **(C)** Detail of inner tube layer in transverse section showing IOP ultrastructure with homogeneous cement, sample DR626 R-4, and scale bar is 10 μm. **(D)** Detail of outer part of fine-grained tube layer showing a grainy appearance, sample DR626 R-4, and scale bar is 5 μm. **(E)** Fine-grained inner tube layer in transverse section showing a transition from a prismatic structure to a grainy/platy structure from left to right, sample DR629 BB, and scale bar is 15 μm. **(F)** Detail of outer coarse-grained tube layer showing spherulitic prismatic (SPHP) ultrastructure, sample DR626 R-4, and scale bar is 10 μm.

not yet been documented from the above region, although there is some similarity in tube ultrastructure (Vinn et al., 2008b). There is also very little information on the occurrence of tabulae in the tubes of modern serpulid species from the genera mentioned above. These "floors" inside serpulid tubes form in response to damage of the posterior tube ending, and are likely produced through the pygidium of the serpulid worm acting as a mold for carbonate precipitation (Hedley, 1958).

Tabulae could thus potentially be formed by a variety of serpulids, and their morphology can be somewhat variable even within a species, thus diminishing their utility taxonomically. Based on the above considerations, the morphology and ultrastructure of the Fossil Hill serpulid tubes is most consistent with the deep-sea genus *Laminatubus*, and we therefore give them the tentative identification of ?*Laminatubus*. The tubes may indeed belong to a now extinct species despite their recent age, or the conditions which led to such a large proliferation of these serpulids may have produced particular tube morphotypes that have not yet been observed in extant species.

Taxa Associated With the Fossil Serpulids

Many of the Fossil Hill samples contained dead benthic mollusk shells in addition to the serpulid tubes **(Supplementary Table S4)**. *E. elongata* was the most common of these associated mollusks, and many specimens in the vibracores (**Figure 6**) and also as rubble on slopes (**Figure 4G**) appeared relatively fresh, with remaining periostracum and a lack of overgrowing authigenic carbonate cement, indicating they were relatively young amongst the rest of the samples (see section "Ages of Fossil Hill Faunas and Authigenic Carbonates"). Other specimens of *E. elongata* in the rock samples were worn and chalky, indicating a greater age. Other bivalve taxa in the Fossil Hill samples included species that are known or strongly suspected to host sulfide-oxidizing chemosymbionts in live specimens. These were the solemyid *Acharax johnsoni* (**Figure 9I**), the vesicomyids *Archivesica packardana* (**Figures 3B**, **9C**), *Phreagena soyoae* (=*P. kilmeri* jr. syn.) (**Figures 4E**, **9A**) and *Pliocardia stearnsii*, the lucinid *Lucinoma aequizonata* (**Figure 9D**), and the thyasirids *Thyasira flexuosa* (**Figure 9E**) and *Axinopsida serricata* (**Figure 9F**). The vesicomyid taxa are all known from methane seep sites further north in Monterey Bay (e.g., Goffredi and Barry, 2002; Johnson et al., 2016). The other bivalve taxa are typical of deep-sea fauna in the East Pacific: the pectinid *Delectopecten vancouverensis* (**Figure 9H**) and the nuculid *Nucula carlottensis* (**Figure 9G**; Coan et al., 2000).

The benthic gastropods in the Fossil Hill samples (**Supplementary Table S4**) are a mixture of taxa occurring at other methane seep sites to the north and south, including the peltospirid *Depressigyra* sp. (**Figure 9J**), the leptodrilid *Lepetodrilus* sp. (**Figure 9U**), the neolepetopsid *Paralepetopsis* sp. (**Figures 9P,Q**), the provannids *Provanna laevis* (**Figure 9K**), *Provanna lomana* (**Figure 9L**) and the pyropeltid *Pyropelta corymba* (**Figure 9T**; Warén and Bouchet, 1993; Levin et al., 2015), and Eastern Pacific deep-sea taxa: the raphitomid *Pleurotomella* sp. and fissurellid *Puncturella rothi* (**Figures 9N,O**; McLean, 1984). The curved shape of the apertures of many of the *Paralepetopsis* sp. and *Pyropelta* spp. specimens (**Figure 9R**), as well as their intimate association with the serpulid tubes in the lightly to heavily mineralized samples strongly indicates they lived on the tubes during life, probably scraping microbial mats from the tube surfaces. This tight association between worm tubes and grazing limpets has been commonly noted from modern and fossil cold seep sites (e.g., Okutani et al., 1992; Jenkins et al., 2007; Saether et al., 2012), although in these cases the tubes are those of siboglinids and not serpulids.

The mollusk taxa associated with the DR630 and DR631 samples are of lower diversity than those in the Fossil Hill samples, and are a sub-set of them (**Supplementary Table S4**). One exception is sample DR631 R-3, which contains specimens of the pteropod *Cavolinia uncinata*, which were derived from the water column and then incorporated into the authigenic carbonates as they formed within the sediments. While 24 taxa were recorded, species richness estimation based on data within **Supplementary Table S4** predicted a minimum of 30–53 fossil species (ICE: 29.5; iChao2: 53.3) from Fossil Hill and associated sites.

Ages of Fossil Hill Faunas and Authigenic Carbonates

Radiocarbon measurements made on the carbonate in the walls of serpulid tubes from several locations around Fossil Hill resulted in a narrow range of calculated ages ranging between 23 and 25 cal ka BP (1000 years before present; **Table 1**). The $\delta^{13}C_{VPDB}$ values of the same samples ranged from −18.06 to −11.01‰. Thus, these Late Pleistocene radiocarbon ages should be treated as a maximum due to potential addition of old carbon effects outlined earlier. Radiocarbon dating of bivalve specimens produced an age similar to that of serpulid tubes for a specimen of *P. soyoae* (23 cal ka BP; **Table 1**), while a shell of the bivalve *E. elongata* was shown to be recent using this technique.

Cements occurring on fossil taxa showed very depleted $\delta^{13}C$ signatures (**Supplementary Table S2**). U-Th dating of cements and fossils was largely consistent with radiocarbon dates, however, U-Th age interpretation was complicated by the fact that most ROV samples yielded a wide range of ages, spanning several tens of ka. Given the size of the samples, such age variation most likely results from some degree of open system behavior through U loss. As a result, the youngest date from each sample was assumed to be representative for the respective locality, provided that its initial ($^{234}U/^{238}U$) activity ratio was within uncertainty of the mean seawater value of 1.1468 (Andersen et al., 2010). Based on this approach we estimate the age of tube-associated authigenic carbonates recovered during dives DR626-630 to be around 17–30 ka (**Table 2**). The older end of this age range is underpinned by statistically equivalent data from three different samples, with only one date from DR626 indicative of a potential older age of around 43 ka. Samples recovered during dive DR631 were analyzed, but returned results consistent with open system behavior, which precluded age interpretation. U-Th dating of cements on bivalve shells from specimens collected on the northern end of Fossil Hill produced ages of approximately 7.1 ka, while carbonate cement on fossil bivalve specimens from the DR630 dive site yielded an age of 20.8 ka (**Table 2**).

DISCUSSION

As serpulid tubes were observed along much of Fossil Hill's extent of over 500 m by 250 m, this mound appears to host one of the largest known accumulations of fossil serpulids, greatly exceeding the dimensions of the Triassic-early Jurassic fossil serpulid reefs

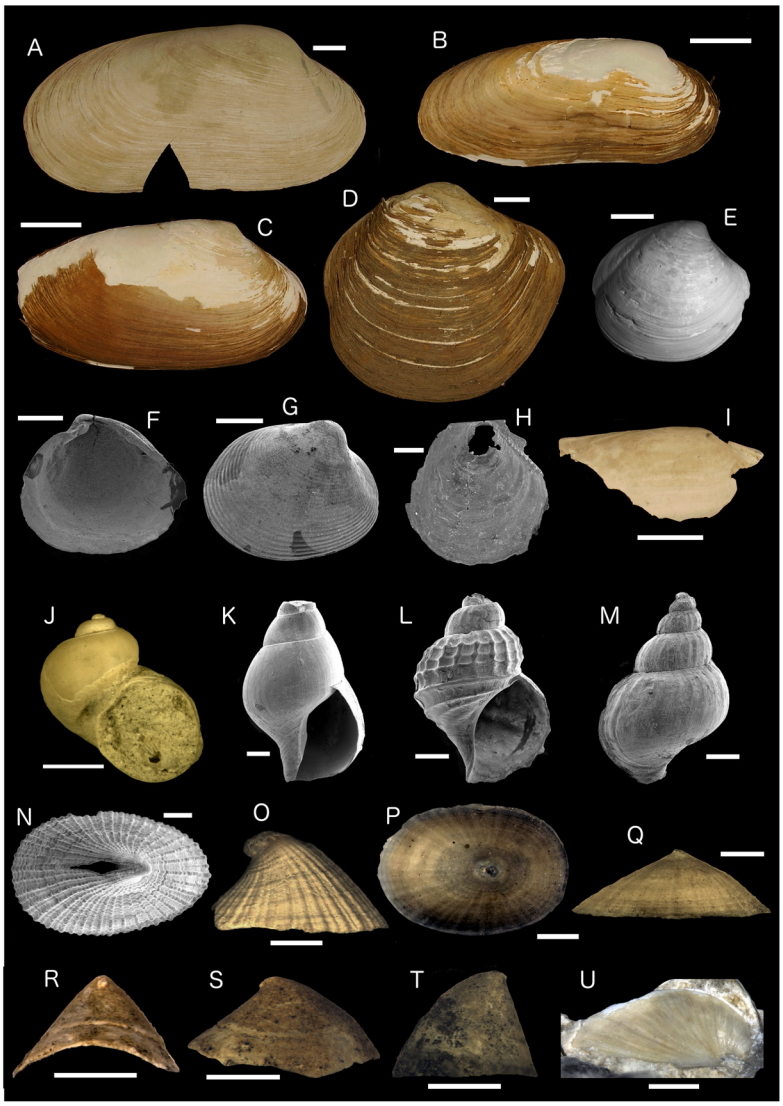

FIGURE 9 | Images of representative bivalves and gastropods from Fossil Hill samples. **(A)** *Phreagena soyoae*, right valve external view, DR627 Bio-2 clam scoop, and scale bar is 10 mm. **(B)** *Ectenagena elongata*, right valve external view, DR626 A-1, and scale bar is 10 mm. **(C)** *Archivesica packardana*, right valve external view, DR626 A-1, and scale bar is 10 mm. **(D)** *Lucinoma aequizonata*, right valve external view, DR629 PSC-61, and scale bar is 10 mm. **(E)** *Thyasira flexuosa*, right valve external view, DR627 (BB), and scale bar is 5 mm. **(F)** *Axinopsida serricata*, right valve internal view, DR627 R-2, SEM, and scale bar is 1 mm. **(G)** *Nucula carlottensis*, left valve external view, DR627 R-2, SEM, and scale bar is 1 mm. **(H)** *Delectopecten vancouverensis*, right valve external view, DR627 BB, SEM, and scale bar is 0.5 mm. **(I)** *Acharax johnsoni*, partial left valve external view, DR627 BIO-2, and scale bar is 10 mm. **(J)** *Depressigyra* sp. apertural view, DR476 A-1, and scale bar is 1 mm. **(K)** *Provanna laevis*, apertural view, DR476 A-1, SEM, and scale bar is 1 mm. **(L)** *Provanna lomana*, apertural view, DR476 A-1, SEM, and scale bar is 1 mm. **(M)** *Provanna* sp., adapertural view, DR476 A-1, SEM, and scale bar is 1 mm. **(N)** *Puncturella rothi*, apical view, DR627 R-2, SEM, and scale bar is 1 mm. **(O)** *Puncturella rothi*, lateral view, DR628 R-3, and scale bar is 2 mm. **(P,Q)** *Paralepetopsis* sp., apical **(P)** and lateral **(Q)** views, DR627 R-2, and scale bars are 1 mm. **(R,S)** *Pyropelta* "low-spired," anterior **(R)** and lateral **(S)** views, DR627 R-2, and scale bars are 1 mm. **(T)** *Pyropelta corymba*, lateral view, DR627 R-2, and scale bar is 1 mm. **(U)** *Lepetodrilus* sp., lateral view, DR629 R-2, and scale bar is 2 mm.

from southern Spain (Braga and Lopez-Lopez, 1989). The Fossil Hill serpulid accumulation is also unusual in being found in deep-sea waters, in association with fossil cold seep faunas, and at a site that still supports an active chemosynthetic biological community with a different assemblage of species. While many mounds characterized by active seepage have been discovered off the coast of California in deep waters (e.g., Orange et al., 2002; Paull et al., 2008, 2015), Fossil Hill and the associated exposures documented in this study are the only examples so far dominated by fossil serpulid tube facies. All of the Fossil Hill serpulid tubes analyzed through radiocarbon dating have maximum ages of 23–24 cal ka BP (**Table 1**) while U-Th dating suggests some tubes are over 16–30 ka old (**Table 2**), demonstrating that this accumulation is remarkably recent in origin and that the species responsible for the accumulation may still be extant.

The current topography of Fossil Hill (**Figure 1C**) appears to be largely a result of differential erosion which has exposed authigenic carbonates and vast quantities of serpulid tube fossils, and this process is likely also responsible for exposing similar facies ∼8 km to the northwest, and ∼300 m to the southeast along the same fault zone as Fossil Hill. Our data are consistent with the formation of the serpulid tube accumulation within deep-sea waters at the Fossil Hill site. This is strongly suggested by the concentrated, well-sorted and oriented nature of the Fossil Hill serpulid tube facies (**Figure 4E**). As only the anterior ends of the tubes were found, there appears to have been some reworking of the deposit. However, based on the considerations above, reworking has likely been spatially constrained to mostly within the Fossil Hill mound area. While Fossil Hill is located in close proximity to the base of the Santa Monica Canyon (**Figure 1**), the mound is situated over 500 m from the main channel in a part of the seabed unlikely to be influenced by canyon transport processes. It therefore appears unlikely that the tubes could have been transported to their current location from shallower, photic zone waters. The morphology of the Fossil Hill tubes is also more consistent with a deep-sea serpulid genus, further suggesting that they likely formed in deep water at the Fossil Hill site.

Is Formation of the Fossil Hill Serpulid Reef Linked to Seepage?

As cold seeps are renowned for supporting greater productivity in comparison to many other deep-sea environments, an apparent explanation for the occurrence of such a large colony of serpulids within a deep-sea cold seep is that its formation is related to productivity from seepage. There are clear indications that active fluid seepage existed at Fossil Hill at the time of tube formation, and may therefore have contributed to the proliferation of these annelids and thus the size of the resulting reef deposit. U-Th dating of MDAC cements on tube surfaces (**Table 2**), and both radiocarbon and U-Th dating of tubes (**Table 1**), indicate that tube formation and fluid seepage were contemporaneous at Fossil Hill during the period 20–25 cal ka BP, while dating of shells additionally suggests that the larger chemosynthetic bivalve species, *Phreagena soyoae*, was also living at the site during this time (**Table 1**). Large vesicomyid bivalves have sulfur-oxidizing bacterial symbionts and require sulfide-rich reducing environments (Krylova and Sahling, 2010), therefore it is likely that the Fossil Hill *P. soyoae* specimens (**Figure 9A**), as well as many of the other fossil fauna (section "Taxa Associated With the Fossil Serpulids"; **Figures 9B–U**) associated with the *?Laminatubus* sp. tubes, would have relied on seeping fluids at the site for their nutrition. In addition, $\delta^{13}C$ values for the fossil serpulid tubes (**Table 1**) also indicate the involvement and importance of methane within the environment at the time the serpulid tubes were forming. The $\delta^{13}C$ values of serpulid tubes are considered to closely resemble those of the waters within which they grew. However vital effects have been reported for this group, whereby tube $\delta^{13}C$ values are shifted to more negative values by 4–7‰ (Videtich, 1986; Lojen et al., 2014). The mechanisms leading to the above effects are however unclear, and a metabolic influence on the low $\delta^{13}C$ values of the Fossil Hill serpulid tubes therefore cannot be ruled out.

While some U-Th measurements suggest slightly older ages for Fossil Hill *?Laminatubus* sp. of 30–43 ka, most U-Th dates, as well as radiocarbon measurements on the above tubes and *P. soyoae* cluster at 16–25 cal ka BP (**Tables 1**, **2**). This may indicate that a discrete event could have occurred during this time period, leading firstly to a vast proliferation of, and subsequently the local extinction of serpulids at the Fossil Hill site. The radiocarbon ages of the tubes approximately coincide with the last glacial maximum (LGM; 20 cal ka BP), during which sea-levels are estimated to have been 110–130 m lower than at present (Lambeck and Chappell, 2001; Bintanja et al., 2005). Intensity of fluid seepage is believed to vary with climatic conditions, in part because ocean warming or a lowering of pressure associated with sea-level changes can lead to dissociation of gas hydrate sequestered near the gas hydrate stability boundary (Kvenvolden, 1988; MacDonald et al., 2003; Buffett and Archer, 2004). For example, the intensity of methane seepage at cold seeps off the coast of mainland Norway and western Svalbard has been linked to isostatic rebound and pulses of sedimentation associated with glaciation during the Late Pleistocene, which altered the stability of gas hydrates (Karstens et al., 2018; Wallmann et al., 2018). Fossil Hill is now at 600 m water depth, near the top of the present methane hydrate stability zone in the Santa Monica Basin (Paull et al., 2008). However, the over 100 m sea-level drop during the LGM likely caused the methane hydrate stability conditions to shift enough for methane hydrate in near-seafloor sediments to decompose, and for methane to be released from sediments. The occurrence of pockmarks, cracks, gullies and caverns on the Fossil Hill mound could indicate the historical presence of gas hydrates that have dissociated, leaving void spaces in the strata and morphologies that suggest seafloor collapse. Methane released from the dissociation of gas hydrate inventoried within near-seafloor sediments, and linked to the LGM sea-level lowstand could have promoted heightened productivity and hence the proliferation of a serpulids as well as chemosynthetic fauna at the Fossil Hill site.

An intriguing question presented by the above scenario is why serpulids, rather than symbiont-bearing chemosynthetic fauna, would have dominated Fossil Hill during a possible period of intense methane seepage during the LGM. It is possible that the Fossil Hill *?Laminatubus* sp. could have possessed chemosynthetic symbionts. While serpulids with such symbiotic associations have not yet been formally described, *Laminatubus* sp. from the Jaco Scar seeps have been found to possess microbial communities on their crowns, and research into the nature of their association with the worms is currently in progress (S. Goffredi, *pers. comm.*). The reason for the extinction of Fossil Hill *?Laminatubus* sp. are however unclear. While there appears to have been active seepage at the Fossil Hill mound during 20–16 ka and 7 ka from MDAC cements (**Table 2**), we cannot at present determine if it was continuous, therefore the possibility exists that the serpulids may have become locally extinct at Fossil Hill during substantial periods of seepage quiescence. Indeed, the bivalve *P. soyoae* appears to also be locally extinct at the Fossil Hill site

despite the occurrence of living populations of these species in nearby seeps (Goffredi and Barry, 2002).

Serpulid Reef Formation and Other Factors

Aspects of the physical environment such as an advantageous position along a fault scarp that provides optimal access to nutrients entrained in water currents, or an unusual composition of the seeping fluid, may also account for why a taxon not deemed to be chemosynthetic was so abundant and co-occurred with seepage at Fossil Hill. Faults can provide conduits for the migration of fluids and are known to be associated with cold seep communities (Zitter et al., 2008), and could additionally have provided serpulids with hard substrate in the form of MDAC for attachment. While other mounds off the Californian coast were generally not found to harbor large abundances of fossil serpulids, serpulid tubes similar to those of Fossil Hill were recovered at the two additional authigenic carbonate outcrops along the approximate trajectory of the San Pedro Basin Fault sampled during dives DR630 and DR631 (**Figure 1**). Therefore, the proximity of fossil serpulid tube facies to the San Pedro Basin Fault may indicate an association between this facies and fault activity. The subset of Fossil Hill U-Th dates that also predate the LGM could suggest that factors other than nutritional benefits from seepage productivity may have been responsible for serpulid reef growth. However, data on historical fault and water current movements are very limited, and it thus remains difficult to account for why serpulids are extinct at the Fossil Hill site today.

It is likely that the formation of the fossil serpulid reef at Fossil Hill is due to a combination of favorable environmental conditions as well as heightened productivity from seepage, particularly ∼20 ka. Serpulid populations in general are known to boom for discrete time periods under which distinct environmental conditions prevail (ten Hove and van den Hurk, 1993), which the Triassic-early Jurassic fossil serpulid reefs from southern Spain (Braga and Lopez-Lopez, 1989) as well as those found near South Georgia (Ramos and San Martín, 1999) demonstrate can occur away from coastal settings in more open, near-deep to deep-sea waters. The large extent of the Fossil Hill deposit, and the known role of serpulids as ecosystem engineers in virtue of reef construction, means that Fossil Hill likely constituted a significant deep-sea habitat for other marine fauna, with the mollusk fauna associated with Fossil Hill serpulids (and the estimated fossil species richness) attesting to this. During the time of active serpulid reef growth during the Late Pleistocene, Fossil Hill could therefore potentially be classed as an "animal forest" (Rossi, 2013; Reyes-Bonilla and Jordán-Dahlgren, 2017) in virtue of providing three-dimensional habitat complexity that can alter physical and biological characteristics of the site.

CONCLUSION

Detailed AUV surveys in combination with extensive ROV sampling have revealed the existence of a massive serpulid paleo-colony dominated by ∼20 cal ka BP tubeworms off southern California. The deposit also contains fossil cold seep faunas and methane-derived carbonates. Similar massive-sized deposits dominated by serpulids have not previously been documented in the deep sea. However, the proportion of the seafloor that has been explored with tools and techniques that allow features like this to be identified is still very small. Further exploration has the potential to shed insight into whether living populations of the Fossil Hill ?*Laminatubus* serpulids may yet still exist within the southern California region, to elucidate the relationship between these tubeworms and fluid seepage, and thus provide answers to the intriguing question as to whether these serpulids may have had chemosymbionts.

DATA AVAILABILITY

All datasets generated for this study are included in the manuscript and/or the **Supplementary Files**.

AUTHOR CONTRIBUTIONS

Samples were collected by CP and RV, with assistance from MG. MM performed radiocarbon dating. DS and DC performed U-Th dating. DWC processed AUV data. LL provided seafloor video mosaic data. MG, CL, and JP analyzed the data and the manuscript was drafted by MG with input from CP, RV, and CL. All authors read and approved the final manuscript.

FUNDING

This study was provided by the David and Lucile Packard Foundation via the Monterey Bay Aquarium Research Institute. MG gratefully acknowledges funding from NERC grants NE/K500847/1 and NE/R000670/1.

ACKNOWLEDGMENTS

We thank the crew of R/V *Western Flyer*, as well as the AUV and ROV *Doc Ricketts* pilots. We are grateful to Ivano Aiello for assistance with SEM at Moss Landing Marine Laboratories, to Hilary Sloane for assistance with stable isotope analyses, to Harry ten Hove, Elena Kupriyanova, Greg Rouse, and Olev Vinn for their advice on the identification of serpulid tubes, and Alexei Ippolitov for advice on SEM examination of serpulid tubes. We also thank Roberto Gwiazda, Esther Sumner, and Shannon Johnson for their assistance with sample collection, as well as Krystle Anderson and Eve Lundsten for their assistance with mapping data and figures. We are also grateful to Jonathan Watson and Mark Sephton for their access to and help with FTIR, to Elena Krylova, Shana Goffredi, Paul Valentich-Scott, Daniel Geiger, Anders Warén, John Taylor, Arie Janssen, and Henry Chaney for their assistance with the identification of mollusk and other taxa, and to

Shannon Johnson for verification of the *E. elongata* identification using DNA sequences from Johnson et al. (2016), as well as additional mollusk identifications. We also thank two reviewers and Harry ten Hove for their valuable comments on the manuscript draft.

SUPPLEMENTARY MATERIAL

The Supplementary Material for this article can be found online at: https://www.frontiersin.org/articles/10.3389/fmars.2019.00115/full#supplementary-material

REFERENCES

Amon, D. J., Gobin, J., Van Dover, C. L., Levin, L. A., Marsh, L., and Raineault, N. A. (2017). Characterization of methane-seep communities in a deep-sea area designated for oil and natural gas exploitation off Trinidad and Tobago. *Front. Mar. Sci.* 4:342. doi: 10.3389/fmars.2017.00342

Andersen, M. B., Stirling, C. H., Zimmermann, B., and Halliday, A. N. (2010). Precise determination of the open ocean 234 U/ 238 U composition. *Geochem. Geophys. Geosyst.* 11:Q12003. doi: 10.1029/2010GC003318

Barbieri, R., Ori, G. G., and Cavalazzi, B. (2004). A silurian cold-seep ecosystem from the middle atlas. *Morocco. Palaios* 19, 527–542. doi: 10.1669/0883-1351(2004)019<0527:ASCEFT>2.0.CO;2

Bastida-Zavala, R. (2008). Serpulids (Annelida: Polychaeta) from the Eastern Pacific, including a brief mention of Hawaiian serpulids. *Zootaxa* 1722, 1–61.

Bianchi, C. N., Aliani, S., and Morri, C. (1995). Present-day serpulid reefs, with reference to an on-going research project on *Ficopomatus enigmaticus*. *Pubblications du Serv. Géologique du Luxemb.* 29, 61–65.

Bintanja, R., van de Wal, R. S. W., and Oerlemans, J. (2005). Modelled atmospheric temperatures and global sea levels over the past million years. *Nature* 437, 125–128. doi: 10.1038/nature03975

Braga, J. C., and Lopez-Lopez, I. R. (1989). Serpulid bioconstructions at the triassic-liassic boundary in southern Spain. *Facies* 21, 1–10. doi: 10.1007/BF02536829

Buffett, B., and Archer, D. (2004). Global inventory of methane clathrate: sensitivity to changes in the deep ocean. *Earth Planet. Sci. Lett.* 227, 185–199. doi: 10.1016/j.epsl.2004.09.005

Caress, D., Thomas, H., Kirkwood, W., McEwen, R., Henthorn, R., Clague, D., et al. (2008). "High-Resolution Multibeam, Sidescan, and Subbottom Surveys Using the MBARI AUV D. Allan B," in *Marine Habitat Mapping Technology for Alaska*, eds J. R. Reynolds and H. G. Greene (Fairbanks: Alaska Sea Grant, University of Alaska Fairbanks), 47–70. doi: 10.4027/mhmta.2008.04

Chao, A., Ma, K. H., Hsieh, T. C., and Chiu, C. H. (2015). *Online Program SpadeR (Species-richness Prediction And Diversity Estimation in R). Program and User's Guide*. Available at: http://chao.stat.nthu.edu.tw/wordpress/software_download/

Chiu, C. H., Wang, Y. T., Walther, B. A., and Chao, A. (2014). An improved nonparametric lower bound of species richness via a modified good–turing frequency formula. *Biometrics* 70, 671–682. doi: 10.1111/biom.12200

Coan, E. V., Valentich Scott, P., and Bernard, F. R. (2000). Bivalve seashells of western North America: marine bivalve mollusks from Arctic Alaska to Baja California. *St. Barbar. Museum Nat. Hist. Monogr.* 2:764.

Crémière, A., Lepland, A., Chand, S., Sahy, D., Condon, D. J., Noble, S. R., et al. (2016). Timescales of methane seepage on the Norwegian margin following collapse of the Scandinavian Ice Sheet. *Nat. Commun.* 7:11509. doi: 10.1038/ncomms11509

Dubilier, N., Bergin, C., and Lott, C. (2008). Symbiotic diversity in marine animals: the art of harnessing chemosynthesis. *Nat. Rev. Microbiol.* 6, 725–740. doi: 10.1038/nrmicro1992

Fisher, M. A., Normark, W. R., Bohannon, R. G., Sliter, R. W., and Calvert, A. J. (2003). Geology of the continental margin beneath Santa Monica Bay, Southern California, from seismic-reflection data. *Bull. Seismol. Soc. Am.* 93, 1955–1983. doi: 10.1785/0120020019

Gardner, J. V., Dartnell, P., Mayer, L. A., and Hughes Clarke, J. E. (2003). Geomorphology, acoustic backscatter, and processes in Santa Monica Bay from multibeam mapping. *Mar. Environ. Res.* 56, 15–46. doi: 10.1016/S0141-1136(02)00323-9

Goffredi, S., and Barry, J. (2002). Species-specific variation in sulfide physiology between closely related vesicomyid clams. *Mar. Ecol. Prog. Ser.* 225, 227–238. doi: 10.3354/meps225227

Hedley, R. H. (1958). Tube formation by *Pomatoceros triqueter* (Polychaeta). *J. Mar. Biol. Assoc.* 37, 315–322. doi: 10.1017/S0025315400023717

Hein, J. R., Normark, W. R., McIntyre, B. R., Lorenson, T. D., and Powell, C. L. II. (2006). Methanogenic calcite, 13C-depleted bivalve shells, and gas hydrate from a mud volcano offshore southern California. *Geology* 34, 108–112. doi: 10.1130/G22098.1

Hoeksema, B. W., and ten Hove, H. A. (2011). Aggregation of the reef-building tube worm *Filogranella elatensis* at Semporna, eastern Sabah, Malaysia. *Coral Reefs* 30:839. doi: 10.1007/s00338-011-0785-8

Hovland, M., and Judd, A. G. (1988). *Seabed Pockmarks and Seepages: Impact on Geology, Biology and the Marine Environment*. London: Graham and Trotman.

Ippolitov, A., Vinn, O., Kupriyanova, E., and Jäger, M. (2014). Written in stone: history of serpulid polychaetes through time. *Mem. Mus. Vic.* 71, 123–159. doi: 10.24199/j.mmv.2014.71.12

Jenkins, R. G., Kaim, A., and Hikida, Y. (2007). Antiquity of the substrate choice among acmaeid limpets from late cretaceous chemosynthesis-based communities. *Acta Palaeontol. Pol.* 52, 369–373.

Johnson, S. B., Krylova, E. M., Audzijonyte, A., Sahling, H., and Vrijenhoek, R. C. (2016). Phylogeny and origins of chemosynthetic vesicomyid clams. *Syst. Biodivers.* 15, 346–360. doi: 10.1080/14772000.2016.1252438

Karstens, J., Haflidason, H., Becker, L. W. M., Berndt, C., Rüpke, L., Planke, S., et al. (2018). Glacigenic sedimentation pulses triggered post-glacial gas hydrate dissociation. *Nat. Commun.* 9:635. doi: 10.1038/s41467-018-03043-z

Kiel, S. (ed.). (2010). *The Vent, and Seep Biota: Aspects from Microbes to Ecosystems*, Vol. 33. Dordrecht: Springer. doi: 10.1007/978-90-481-9572-5

Kiel, S., Sami, M., and Taviani, M. (2018). A serpulid-*Anodontia*-dominated methane-seep deposit from the miocene of northern italy. *Acta Palaeontol. Pol.* 63, 569–577. doi: 10.4202/app.00472.2018

Krylova, E. M., and Sahling, H. (2010). Vesicomyidae (Bivalvia): current taxonomy and distribution. *PLoS One* 5:e9957. doi: 10.1371/journal.pone.0009957

Kupriyanova, E. K. (1999). The taxonomic status of *Serpula* cf. columbiana Johnson, 1901 from the American and Asian coasts of the North Pacific ocean. *Ophelia* 50, 21–34. doi: 10.1080/00785326.1999.10409386

Kupriyanova, E. K., Macdonald, T. A., and Rouse, G. W. (2006). Phylogenetic relationships within Serpulidae (Sabellida, Annelida) inferred from molecular and morphological data. *Zool. Scr.* 35, 421–439. doi: 10.1186/1471-2148-9-189

Kvenvolden, K. A. (1988). Methane hydrates and global climate. *Global Biogeochem. Cycles* 2, 221–229. doi: 10.1029/GB002i003p00221

Lambeck, K., and Chappell, J. (2001). Sea level change through the last glacial cycle. *Science* 292, 679–686. doi: 10.1126/science.1059549

Lee, S.-M., and Chao, A. (1994). Estimating population size via sample coverage for closed capture-recapture models. *Biometrics* 50, 88–97. doi: 10.2307/2533199

Levin, L. A., Mendoza, G. F., Grupe, B. M., Gonzalez, J. P., Jellison, B., Rouse, G., et al. (2015). Biodiversity on the rocks: macrofauna inhabiting authigenic carbonate at costa rica methane seeps. *PLoS One* 10:e0131080. doi: 10.1371/journal.pone.0131080

Levin, L. A., Orphan, V. J., Rouse, G. W., Rathburn, A. E., Ussler, W., Cook, G. S., et al. (2012). A hydrothermal seep on the Costa Rica margin: middle ground in a continuum of reducing ecosystems. *Proc. R. Soc. B Biol. Sci.* 279, 2580–2588. doi: 10.1098/rspb.2012.0205

Loftus, E., Rogers, K., and Lee-Thorp, J. (2015). A simple method to establish calcite:aragonite ratios in archaeological mollusc shells. *J. Quat. Sci.* 30, 731–735. doi: 10.1002/jqs.2819

Lojen, S., Cukrov, M., and Cukrov, N. (2014). Variability of stable isotope fingerprints of the serpulid *Ficopomatus enigmaticus* within a permanently stratified estuary: implications for (palaeo)environmental interpretations. *Estuaries Coast.* 37, 436–448. doi: 10.1007/s12237-013-9685-1

MacDonald, I. R., Sager, W. W., and Peccini, M. B. (2003). Gas hydrate and chemosynthetic biota in mounded bathymetry at mid-slope hydrocarbon

seeps: northern Gulf of Mexico. *Mar. Geol.* 198, 133–158. doi: 10.1016/S0025-3227(03)00098-7

McLean, J. H. (1984). New species of northeast pacific archaeogastropods. *Veliger* 26, 233–239.

Mix, A. C., Lund, D. C., Pisias, N. G., Bodén, P., Bornmalm, L., Lyle, M., et al. (1999). "Rapid climate oscillations in the Northeast Pacific during the last deglaciation reflect Northern and Southern Hemisphere sources," in *Mechanisms for Global Climate Change at Millennial Time Ccales*, eds P. Clark, R. S. Webb, and L. D. Keigwin (Washington, D. C: American Geophysical Union), 127–148. doi: 10.1029/GM112p0127

Nobuhara, T., Onda, D., Kikuchi, N., Kondo, Y., Matsubara, K., Amano, K., et al. (2008). Lithofacies and fossil assemblages of the upper cretaceous sada limestone, Shimanto City, Kochi Prefecture, Shikoku, Japan. *Fossils* 84, 47–60.

Nobuhara, T., Onda, D., Sato, T., Aosawa, H., Ishimura, T., Ijiri, A., et al. (2016). Mass occurrence of the enigmatic gastropod *Elmira* in the late cretaceous sada limestone seep deposit in southwestern Shikoku, Japan. *PalZ* 90, 701–722. doi: 10.1007/s12542-016-0326-4

Normark, W. R., Hein, J. R., Powell, C. L. I. I., Lorenson, T. D., Lee, H. J., and Edwards, B. D. (2003). Methane hydrate recovered from a mud volcano in santa monica basin, offshore southern California. *EOS Trans. Am. Geophys. Union* 84, 51B–0855B.

Okutani, T., Tsuchida, E., and Fujikura, K. (1992). Five bathyal gastropods living within or near the *Calyptogena*-community of the Hatsushima Islet, Sagami Bay. *Venus* 51, 137–148.

Olu, K., Duperret, A., Sibuet, M., Foucher, J., and Fiala-Medoni, A. (1996a). Structure and distribution of cold seep communities along the Peruvian active margin: relationship to geological and fluid patterns. *Mar. Ecol. Prog. Ser.* 132, 109–125. doi: 10.3354/meps132109

Olu, K., Sibuet, M., Harmegnies, F., Foucher, J., and Fiala-Medoni, A. (1996b). Spatial distribution of diverse cold seep communities living on various diapiric structures of the southern Barbados prism. *Prog. Oceanogr.* 38, 347–376. doi: 10.1016/S0079-6611(97)00006-2

Orange, D. L., Yun, J., Maher, N., Barry, J., and Greene, G. (2002). Tracking California seafloor seeps with bathymetry, backscatter and ROVs. *Cont. Shelf Res.* 22, 2273–2290. doi: 10.1016/S0278-4343(02)00054-7

Paull, C. K., Caress, D. W., Thomas, H., Lundsten, E., Anderson, K., Gwiazda, R., et al. (2015). Seafloor geomorphic manifestations of gas venting and shallow subbottom gas hydrate occurrences. *Geosphere* 11, 491–513. doi: 10.1130/GES01012.1

Paull, C. K., Chanton, J., Neumann, A. C., Coston, J. A., Martens, C. S., and Showers, W. (1992). Indicators of methane-derived carbonates and chemosynthetic organic carbon deposits: examples from the Florida Escarpment. *Palaios* 7, 361–375. doi: 10.2307/3514822

Paull, C. K., Martens, C. S., Chanton, J. P., Neumann, A. C., Coston, J., Jull, A. J. T., et al. (1989). Old carbon in living organisms and young CaCO3 cements from abyssal brine seeps. *Nature* 342, 166–168. doi: 10.1038/342166a0

Paull, C. K., Normark, W. R., Ussler, W., Caress, D. W., and Keaten, R. (2008). Association among active seafloor deformation, mound formation, and gas hydrate growth and accumulation within the seafloor of the Santa Monica Basin, offshore California. *Mar. Geol.* 250, 258–275. doi: 10.1016/j.margeo.2008.01.011

Peckmann, J., Thiel, V., Michaelis, W., Clari, P., Gaillard, C., Martire, L., et al. (1999a). Cold seep deposits of Beauvoisin (Oxfordian, southeastern France) and Marmorito (Miocene, northern Italy): microbially induced authigenic carbonates. *Int. J. Earth Sci.* 88, 60–75. doi: 10.1007/s005310050246

Peckmann, J., Walliser, O. H., Riegel, W., and Reitner, J. (1999b). Signatures of hydrocarbon venting in a middle devonian carbonate mound (Hollard Mound) at the Hamar Laghdad (Antiatlas Morocco). *Facies* 40, 281–296. doi: 10.1007/BF02537477

Pohlman, J. W., Bauer, J. E., Waite, W. F., Osburn, C. L., and Chapman, N. R. (2011). Methane hydrate-bearing seeps as a source of aged dissolved organic carbon to the oceans. *Nat. Geosci.* 4, 37–41. doi: 10.1038/ngeo1016

Prouty, N. G., Sahy, D., Ruppel, C. D., Roark, E. B., Condon, D., Brooke, S., et al. (2016). Insights into methane dynamics from analysis of authigenic carbonates and chemosynthetic mussels at newly-discovered Atlantic Margin seeps. *Earth Planet. Sci. Lett.* 449, 332–344. doi: 10.1016/j.epsl.2016.05.023

R Core Team (2014). *R: A Language and Environment for Statistical Computing*. Vienna: R Foundation for Statistical Computing.

Ramos, A., and San Martín, G. (1999). On the finding of a mass occurrence of *Serpula narconensis* Baird, 1885 (Polychaeta, Serpulidae) in South Georgia (Antarctica). *Polar Biol.* 22, 379–383. doi: 10.1007/s003000050432

Reish, D. J., and Mason, A. Z. (2003). Radiocarbon dating and metal analyses of fossil and living tubes of *Protula* (Annelida: Polychaeta). *Hydrobiologia* 496, 371–383. doi: 10.1023/A:1026186024182

Reyes-Bonilla, H., and Jordán-Dahlgren, E. (2017). "Caribbean Coral Reefs: Past, Present, and Insights into the Future," in *Marine Animal Forests*, eds S. Rossi, L. Bramanti, A. Gori, and C. Orejas (Cham: Springer), doi: 10.1007/978-3-319-17001-5_2-1

Rossi, S. (2013). The destruction of the 'animal forests' in the oceans: towards an over-simplification of the benthic ecosystems. *Ocean Coast. Manag.* 84, 77–85. doi: 10.1016/j.ocecoaman.2013.07.004

Ryan, H. F., Conrad, J. E., Paull, C. K., and McGann, M. (2012). Slip rate on the San Diego trough fault zone, inner California Borderland, and the 1986 Oceanside earthquake swarm revisited. *Bull. Seismol. Soc. Am.* 102, 2300–2312. doi: 10.1785/0120110317

Saether, K. P., Little, C. T. S., Marshall, B. A., and Campbell, K. A. (2012). Systematics and palaeoecology of a new fossil limpet (Patellogastropoda: Pectinodontidae) from Miocene hydrocarbon seep deposits, East Coast Basin, North Island, New Zealand with an overview of known fossil seep pectinodontids. *Molluscan Res.* 32, 1–15.

Sanfilippo, R., Vertino, A., Rosso, A., Beuck, L., Freiwald, A., and Taviani, M. (2013). *Serpula* aggregates and their role in deep-sea coral communities in the southern Adriatic Sea. *Facies* 59, 663–677. doi: 10.1007/s10347-012-0356-7

Schwindt, E., Bortolus, A., and Iribarne, O. O. (2001). Invasion of a reef-builder polychaete: direct and indirect impacts on the native benthic community structure. *Biol. Invasions* 3, 137–149. doi: 10.1023/A:1014571916818

Stuiver, M., and Polach, H. A. (1977). Discussion: reporting of 14C data. *Radiocarbon* 19, 355–363. doi: 10.1017/S0033822200003672

Stuiver, M., Reimer, P. J., and Reimer, R. W. (2018). *CALIB 7.1 [WWW program]*. Available at: http://calib.org, accessed 2018-9-26

Taylor, P. D., and Vinn, O. (2006). Convergent morphology in small spiral worm tubes ('*Spirorbis*') and its palaeoenvironmental implications. *J. Geol. Soc. London.* 163, 225–228. doi: 10.1144/0016-764905-145

ten Hove, H. (1979). "Different causes of mass occurrence in serpulids," in *Biology and Systematics of Colonial Organisms*, eds G. Larwood and B. R. Rosen (London: Academic Press), 281–298.

ten Hove, H., and van den Hurk, P. (1993). A review of Recent and fossil serpulid 'reefs'; actuopalaeontology and 'Upper Malm' serpulid limestones in NW Germany. *Geol. en Mijnb* 72, 23–67.

ten Hove, H., and Zibrowius, H. (1986). Laminatubus alvini gen. et sp. n. and Protis hydrothermica sp. n. (Polychaeta, Serpulidae) from the bathyal hydrothermal vent communities in the eastern Pacific. *Zool. Scr.* 15, 21–31. doi: 10.1111/j.1463-6409.1986.tb00205.x

Videtich, P. E. (1986). Stable-isotope compositions of serpulids give insights to calcification processes in marine organisms. *Palaios* 1, 189–193. doi: 10.2307/3514514

Vinn, O. (2005). The tube ultrastructure of serpulids (Annelida, Polychaeta) Pentaditrupa subtorquata, Cretaceous, and Nogrobs cf. vertebralis, Jurassic, from Germany. *Proc. Estonian Acad. Sci. Geol.* 54, 260–265.

Vinn, O. (2008). Tube ultrastructure of the fossil genus *Rotularia* DeFrance, 1827 (Polychaeta, Serpulidae). *J. Paleontol.* 82, 206–212. doi: 10.1666/06-125.1

Vinn, O., Hryniewicz, K., Little, C. T. S., and Nakrem, H. A. (2014). A Boreal serpulid fauna from Volgian-Ryazanian (latest Jurassic-earliest Cretaceous) shelf sediments and hydrocarbon seeps from Svalbard. *Geodiversitas* 36, 527–540. doi: 10.5252/g2014n4a2

Vinn, O., Jäger, M., and Kirsimäe, K. (2008a). Microscopic evidence of serpulid affinities of the problematic fossil tube *Serpula etalensis* from the Lower Jurassic of Germany. *Lethaia* 41, 417–421. doi: 10.1111/j.1502-3931.2008.00093.x

Vinn, O., ten Hove, H., Mutvei, H., and Kirsimae, K. (2008b). Ultrastructure and mineral composition of serpulid tubes (Polychaeta, Annelida). *Zool. J. Linn. Soc.* 154, 633–650. doi: 10.1111/j.1096-3642.2008.00421.x

Vinn, O., Kupriyanova, E. K., and Kiel, S. (2013). Serpulids (Annelida, Polychaeta) at Cretaceous to modern hydrocarbon seeps: ecological and evolutionary patterns. *Palaeogeogr. Palaeoclimatol. Palaeoecol.* 390, 35–41. doi: 10.1016/j.palaeo.2012.08.003

Wagner, J. K., McEntee, M. H., Brothers, L. L., German, C. R., Kaiser, C. L., Yoerger, D. R., et al. (2013). Cold-seep habitat mapping: high-resolution spatial characterization of the blake ridge diapir seep field. *Deep Sea Res. II* 92, 183–188. doi: 10.1016/j.dsr2.2013.02.008

Wallmann, K., Riedel, M., Hong, W. L., Patton, H., Hubbard, A., Pape, T., et al. (2018). Gas hydrate dissociation off Svalbard induced by isostatic rebound rather than global warming. *Nat. Commun.* 9:83. doi: 10.1038/s41467-017-02550-9

Warén, A., and Bouchet, P. (1993). New records, species, genera, and a new family of gastropods from hydrothermal vents and hydrocarbon seeps. *Zool. Scr.* 22, 1–90. doi: 10.1111/j.1463-6409.1993.tb00342.x

Zitter, T. A. C., Henry, P., Aloisi, G., Delaygue, G., Çagatay, M. N., Mercier de Lepinay, B., et al. (2008). Cold seeps along the main marmara fault in the sea of marmara (Turkey). *Deep Sea Res. Part I Oceanogr. Res. Pap.* 55, 552–570. doi: 10.1016/j.dsr.2008.01.002

Conflict of Interest Statement: The authors declare that the research was conducted in the absence of any commercial or financial relationships that could be construed as a potential conflict of interest.